

MODELLING FIBROUS MATERIALS AS A LARGE DEFORMATION, NON-
LOCAL AND NON-LINEAR TRUSS NETWORK

A Thesis

by

JAGANATH GANGADARAN

Submitted to the Office of Graduate and Professional Studies of
Texas A&M University
in partial fulfillment of the requirements for the degree of

MASTER OF SCIENCE

Chair of Committee,	Arun Srinivasa
Committee Members,	Anastasia Muliana
	Terry Creasy
Head of Department,	Andreas Polycarpou

December 2015

Major Subject: Mechanical Engineering

Copyright 2015 Jaganath Gangadaran

ABSTRACT

Modelling fibrous networks is crucial to understand the mechanics of soft materials like ligaments, connective tissues, alveolus sac and nonwoven fabrics. Simulation of these fibrous networks has been typical restricted to modelling them as a local continuum where the filaments are connected to the nearest neighbors. These methods do not capture the actual microstructure of the fibers, where there are non-local connections. Non-local connection refers to long fibers that connect cross-links that are not near each other. This thesis proposes modelling fibrous networks as a truss system with large deformation. A network of trusses will be able to capture the microstructure of fibrous networks more accurately. The strain energy of the truss system will be assembled and solved by minimizing the total potential energy of the system. Modelling of local and non-local fibrous networks have been done in this work.

The random fibrous networks were generated from the probability distribution of cross-links identified in the SEM (Scanning Electron Microscope) images of the fibrous material. The nodes were then connected by truss elements based on the probability distribution of number of nodal connections as a function of distance. Various other methods for developing random fibrous network have also been proposed in this work.

A pulmonary alveolus sac of a human lung was modelled as a case of a local system. It was found that there were no significant differences between results obtained if linear response of fibers was used instead of non-linear response. Also, no significant

differences were exhibited between approximating the non-local system as a continuum versus modelling it as a network of trusses.

A non-local system of type 1 collagen fiber was generated as a random truss network. It was found that there were significant differences between results obtained if linear response of fibers was used instead of non-linear. The deformation mode of non-local fibrous network was different for linear and non-linear. Also, significant differences were exhibited between approximating the non-local system as a continuum versus modelling it as a network of trusses.

ACKNOWLEDGEMENTS

I would like to express my deepest gratitude to my committee chair, Dr. Arun Srinivasa, for his support, invaluable guidance and constant encouragement throughout the time spent conducting research. Without his patience and council, this thesis would have been an overwhelming pursuit. I would like to thank Dr. Muliana and Dr. Creasy for agreeing to serve on my committee.

Finally, I would like thank my mother D. Vathsala and my father R.Gangadaran for their constant encouragement and support during these years spent pursuing my graduate studies.

TABLE OF CONTENTS

	Page
ABSTRACT	ii
ACKNOWLEDGEMENTS	iv
TABLE OF CONTENTS	v
LIST OF FIGURES.....	vii
CHAPTER I INTRODUCTION AND LITERATURE REVIEW	1
I.1 Literature Review.....	3
I.1.1 Experimental Data Reviewed.....	3
I.1.2 Previous Models Developed to Study Fibrous Networks	5
I.2 Proposed Work.....	8
CHAPTER II FIBROUS MATERIAL MODELLED AS A TRUSS NETWORK.....	11
II.1 Generating Nodal Locations of Random Fibrous Network.....	11
II.1.1 Homogenous Nodal Location Generation	13
II.1.2 Inhomogeneous Nodal Location Generation	13
II.2 Generating Nodal Locations of Random Fibrous Network.....	15
CHAPTER III ENERGY FORMULATION FOR THE TRUSS SYSTEM AND FINDING THE AVERAGE DEFORMATION GRADIENT	20
III.1 Principle of Minimum Potential Energy	20
III.2 Relation between Engineering Strain and Green Lagrange Finite Deformation ..	21
III.3 Strain Energy Formulation for a Truss (2-D).....	23
III.3.1 Strain Energy of the Truss.....	24
III.4 Strain Energy for Linear and Non-Linear Response.....	27
III.5 Finding Average Deformation Gradient	29
CHAPTER IV DEFORMATION OF A LOCAL SYSTEM	31
IV.1 Locally Connected Fibrous Network of Pulmonary Alveolus Sac	31
IV.1.1 Modelling an Alveolus Sac Elastic Support as a Dodecahedron	32
IV.2 Comparison between Deformation in Linear and Non-Linear Systems	35
IV.3 Comparison between Deformation Predicted by Truss Network and Approximating as a Continuum	36

CHAPTER V DEFORMATION OF A NON- LOCAL SYSTEM.....	38
V.1 Comparison between Deformation in Linear and Non-Linear System Reponses.	38
V.2 Comparison between Deformation Predicted by Truss Network and Approximating as a Continuum	40
CHAPTER VI CONCLUSION.....	44
REFERENCES	46
APPENDIX A	49
APPENDIX B	56

LIST OF FIGURES

	Page
Figure 1: (a) SEM of nonwoven geotextile SF32 [9] to illustrate an example of random fibrous network. (b) SEM of a toad's lung inner surface [10], the septa(S) (made up of collagen and elastin fibers) that divide the alveolus sac from each other is in form of a polygonal network. (b) Is an example of well-defined fibrous networks that can be modelled by simple geometrical objects.	2
Figure 2: Stress-Strain curve of collagen (2 mg/mL, pH 7.4) matrix of 20x40 mm dog-bone specimen, tested at tensile strain rate of 38.5 percent/min [12]......	4
Figure 3: (a) Schematic representation of the fibrous network, comprised of linear response filaments and matrix. (b) Shows the discretized planar model surface, the red dots shows the fibrous filaments that were developed along the edges of the tetrahedral elements passing through the planar surface.	6
Figure 4: Real (left) and simulated (right) topologies of Poly (ester-urethane) urea [20]. The fiber intersections were identified in the real image (shown in middle with purple color). The fiber connections were performed on the identified nodes using Delaunay triangulation algorithm.	7
Figure 5: (a) Shows the SEM image of pulmonary alveolus sac. (b) Septal stress values in lung region of PTP (Pulmonary Transmissions Pressure) of 9 cm on deflation. The fibers were modelled as linear, fibers with unstressed length were omitted in the simulation [15]. This is a typical simulation of well-defined fibrous network as polygons. A single support will be modelled in this thesis in 3-D as a dodecahedron. *Large alveoli lacking cross bridges.....	9
Figure 6: SEM of type 1 collagen fiber [22]. The red box represents the characteristic length of the matrix to be simulated. Locations where the fibers overlap are modelled as contact points. Fibers originating from these contact points overlapping other fibers in the model are assumed to be sliding over each other without friction.	12
Figure 7: Random nodes generated from the PDF of the nodal connections identified in the SEM of fibrous network. (a) Shows originally identified nodes. (b) Shows nodes generated from (a).....	14
Figure 8: Probability distribution of points identified in 7(a). Kernel Epanechnikov probability distribution was found the best fit for the given data.	14

Figure 9: 1000 points generated from the probability distribution of points shown in Figure 8. The inhomogeneity in the distribution can clearly be seen as there are few points when $x=1$	15
Figure 10: Flow charts developed for the two major categories for connecting random nodes generated.	16
Figure 11: Probability distribution of nodal connections as a function of distance for nodes developed in 7(b).....	17
Figure 12: Non-local fibrous network developed from the SEM (Scanning Electron Microscope) image of type 1 collagen fiber in Figure 6. (a) Shows homogenous and anisotropic connection. (b) Shows homogenous and isotropic connection. The nodal points generated were inhomogeneous.	18
Figure 13: 2-D Truss with 3 members in reference and current configuration.	23
Figure 14: Time taken to solve fibrous network along with the number of elements.....	26
Figure 15: Linear and non-linear curve fit using odd polynomials of stress-strain data of individual collagen fibrils.....	28
Figure 16: Alveoli structure, red bands show the elastic fiber support [13].	32
Figure 17: Elastic support of alveolus modelled as a dodecahedron.	33
Figure 18: Repose of dodecahedron upon applying radially expanding forces from the centroid. Filaments in red experience higher strain than filaments in blue.	33
Figure 19: Macroscopic vs microscopic stress-strain of dodecahedron.....	34
Figure 20: Maximum microscopic strain for linear and non-linear responses.....	35
Figure 21: Shape of dodecahedron deformed by minimizing the strain energy (blue line) and approximating as a local continuum (red line).	36
Figure 22: Percentage of fibers failing (strain>30%) given an applied load for linear and non-linear response.	39
Figure 23: Deformation mode of linear (a) and non-linear (b) response given a tensile load of $7.45e-4N$	40
Figure 24: Deformed shape of dodecahedron by minimizing the strain energy (blue line) and approximating as a local continuum (red line).	41

Figure 25: Plot of average strain calculated using the deformation gradient vs actual strain.42

CHAPTER I

INTRODUCTION AND LITERATURE REVIEW

Fibrous material networks are composites with filaments embedded in a soft base matrix [1]. These materials are commonly encountered in the field of engineering and biological systems. For example, in field of engineering, metallic foams (materials with high porosities levels) are being sought after for their application in building light weight structure. A wider list of fibrous material incorporate day to day common material like wood, cloth polymer like nonwoven cloth and biological tissues. In the proposed thesis, the following fibrous networks materials will be modelled. 1) Soft tissues like collage fiber, it is the major load carrying element in wide variety of organs. 2) Nonwoven fabrics, they are fabric materials like felt that are made up of long fibers.

The mechanical behavior of collagen fiber is characterized by low-stiffness initial region, followed by high stiffness region[2].The deformation is different at macroscopic levels and microscopic levels, for example, given a macroscopic deformation (sample characteristic length), the deformation (axial strain) at microscopic level (fiber filament scale) can be larger than the macroscopic deformation [3]. This characteristic of fibers network leads to injuries like grade 1 ligament tear [4], wear and tear of synovial joints causes fibers in cartilage to stiffen causing arthritis [5]. Other prominent examples on the importance of understanding mechanics of fibrous structures are: Malignant breast cancerous tumor tissues were found to be stiffer than the surrounding tissues [6], amniotic membrane used in skin grafts are primarily composed of collagen fibers [7] and alveolus

sac support made up of polygon shaped fibrous network faces risk of pressure injuries from deep sea diving [8]. Current models developed to study fibrous networks will be examined in the literature review.

The structure of fibrous network can broadly classified into two categories:

- 1) Random fibrous network (nonwoven fabrics and collagen fibers found in connective tissues of our body) as shown below in Figure 1 (a).
- 2) Fibrous networks that can be approximated by simple geometric objects (pulmonary alveolus elastic fibers that can be approximated as polygons) as shown below in Figure 1(b).

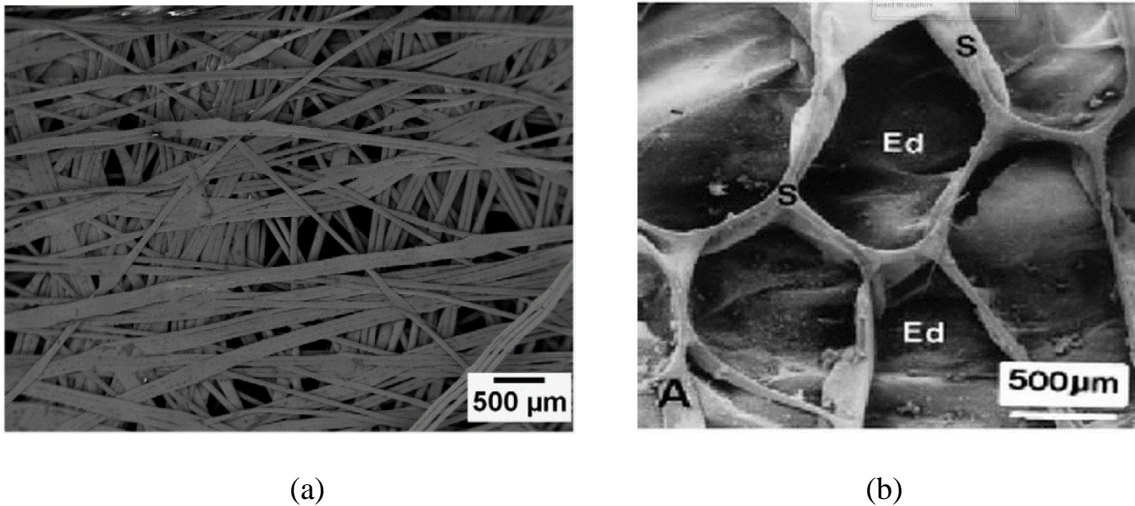


Figure 1: (a) SEM of nonwoven geotextile SF32 [9] to illustrate an example of random fibrous network. (b) SEM of a toad's lung inner surface [10], the septa(S) (made up of collagen and elastin fibers) that divide the alveolus sac from each other is in form of a polygonal network. (b) Is an example of well-defined fibrous networks that can be modelled by simple geometrical objects.

I.1 Literature Review

In this section, major papers pertaining to this area will be listed below and a more detailed discussion of these papers will follow.

A comprehensive guide to fibrous material, their classification and experimental techniques can be found in [1]. A recent review paper of fibrous materials and their mechanical properties can be found in [3]. Papers [9, 11-15] consists of various experimental research done to understand the mechanics of fibrous network. Papers [16-20] consists of the various models developed to study fibrous network.

I.1.1 Experimental Data Reviewed

Tensile stress-strain experiments were performed for nonwoven fabric in [9]. This experiment performed on geotextile made of polypropylene fibers (SF32, commercial name). The fibers were of diameter 60 μm . Tensile experiment was performed on a matrix of 100x 200 mm^2 . The fibers showed a strain of 200% given a strain of 250 MPa. Experimental data of rat lung microscopic alveolar wall elasticity and macroscopic mechanical properties of the whole lung is done in [11]. Three-dimensional tensile properties of ECM (Extracellular Matrices) collagen is done in [12]. Figure 2 below shows the stress strain response of the collagen matrix. Another, collagen fiber data from human skin was presented in [13], the human skin had a maximum strain of 100% when the applied force was 6 MPa. Alveolar septal strain, stress data was measured in [14]. This

experiment was performed in vitro, the stress-strain relations were measured for a lung tissue of 200 μm and a maximum stain of 60% was measured with a failure stress of $2.0 \times 10^5 \frac{\text{dyn}}{\text{cm}^2}$.

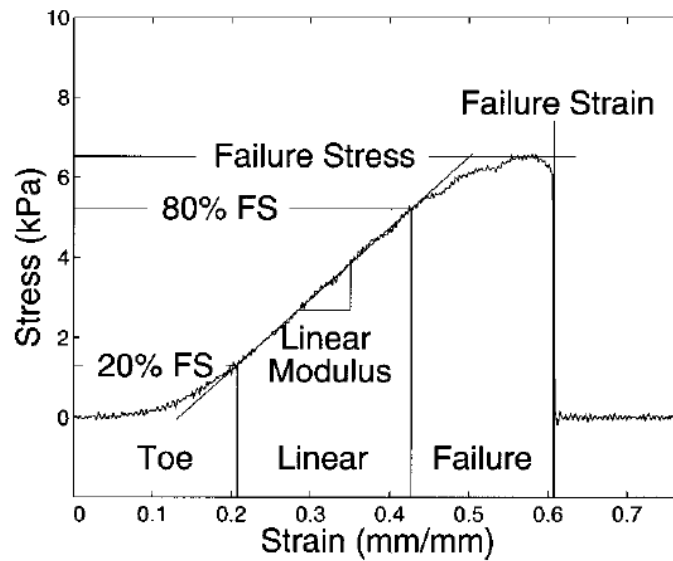


Figure 2: Stress-Strain curve of collagen (2 mg/mL, pH 7.4) matrix of 20x40 mm dog-bone specimen, tested at tensile strain rate of 38.5 percent/min [12].

The data for type 1 collagen fiber was taken from [15]. The measurements were made with filaments with diameters ranging from 150-470 nm and gauge length ranging from 5-21 μm taken from isolated sea cucumber using a MEMS based method (Micro-Electro-Mechanical-Systems). The filaments showed strain up to 30% given a stress of 200Mpa.

1.1.2 Previous Models Developed to Study Fibrous Networks

In [16], a model was developed to study the mechanical response of a nonwoven fabric. The key problem in the paper was to understand fracture mechanics and progressive fracture that lead to the failure of the entire network. In this paper, all individual fibers were considered to have linearly elastic properties. In the reported results, however, although the individual fibers were linear, they experienced large deformations (up to 100%). Another discrepancy noted was, on application of small macroscopic deformation, the deformation at microscopic level was large (when applied macroscopic strain was 10%, some fibers experienced strain of up to 40%).

Work was done in [17], on nonlinear fibrous networks (Air-Lite polyester quilt batting). Where, the microscopic behavior of the fiber was described by theory of Elastica. However, this non-linear fibrous network theory focused on fibril's where strain greater than 5% was considered as a failure of the fibril. Carbon fiber composites are an example of material with high stiffness fibrils.

In [18], the strain energy of the fiber network was taken as a sum of individual fibers are solved linearly using a FEM (Finite element Method) solver. The individual fibers were modelled both as linear Euler-Bernoulli and Timoshenko beams.

In [19], the mechanical behavior of three-dimensional cross linked fibrous network was studied in this work. The model consists of linear elastic fibers with deformation only in axial mode. The volume of the three-dimensional fibrous network was discretized using tetrahedral elements assigned linear elastic matrix properties. The fibers were assumed to

be along the edges of the tetrahedral elements. The model was deformed by imposing displacement boundary conditions. Simulations in this work was only done up to 10% strain. Figure 3 below shows the three-dimensional fibrous network and the model planar surface showing the discretized matrix.

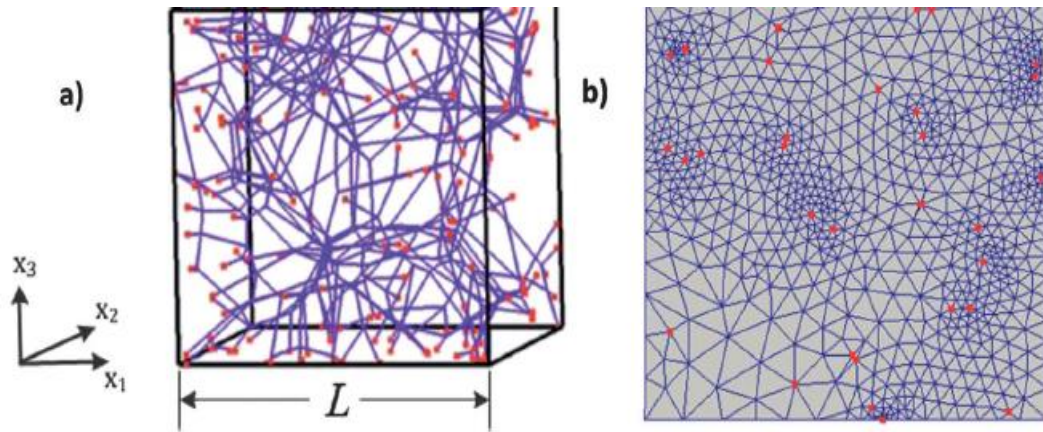


Figure 3: (a) Schematic representation of the fibrous network, comprised of linear response filaments and matrix. (b) Shows the discretized planar model surface, the red dots shows the fibrous filaments that were developed along the edges of the tetrahedral elements passing through the planar surface.

In [20], the mechanical behavior of elastomer membrane (Elastomeric electro spun polyurethane) were simulated by quantifying the actual fibrous geometries. Simulation were performed on experimentally derived fibrous geometries which was developed using image analysis. The effect of fiber intersection, connectivity and orientation on the macro-mechanics of the fibrous network were studied in this paper. Figure 4 below shows the quantification procedure used to quantify the fibrous microstructure from the actual SEM (Scanning Electron Microscope) image to the corresponding simulated topology.

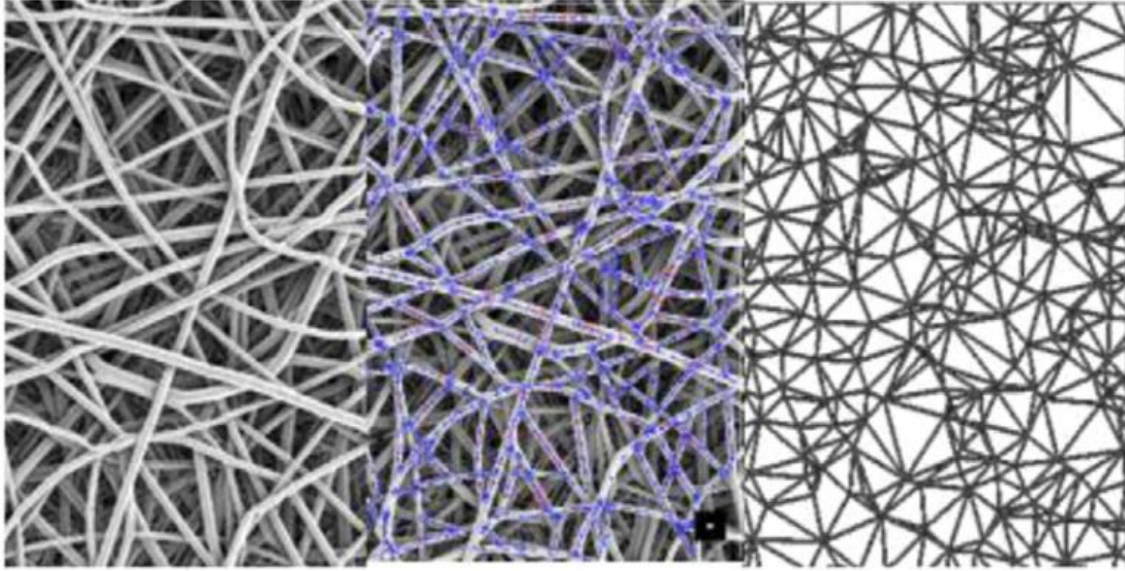


Figure 4: Real (left) and simulated (right) topologies of Poly (ester-urethane) urea [20]. The fiber intersections were identified in the real image (shown in middle with purple color). The fiber connections were performed on the identified nodes using Delaunay triangulation algorithm.

An incompressible Yeoh strain energy of form shown below in equation 1.1 was used. The model was implemented using Abaqus Finite Element Solver.

$$\Psi = \sum_{i=1}^3 C_{i0} (I_c - 3)^i \quad 1.1$$

where, C_{i0} represents the material parameter and I_c first invariant of right Cauchy Green Stretch Tensor. The strain energy assumed the model was isotropic and incompressible, however in the paper, the same strain energy was used for an anisotropic fibrous network.

I.2 Proposed Work

In the models discussed in section I.1.2, deformation due to non-local response is not taken into account. The constitutive equations developed for these models are based on classical continuum mechanics. In classical continuum mechanics, for determining the stress at a given point, the contribution of stress from elements outside an arbitrary neighborhood are disregarded [21]. However, in case of random fibrous network as shown in Figure 4, the connections are non-local (there are long fibers going from one end of the matrix to the other), hence local continuum deformation models are not suitable for modelling random fibrous network. This is reflected in the simulated topologies of fibrous network shown in Figure 3 (b) and 4, where the resulting topologies are devoid of any non-local connections (absence of long fibers) and each fiber is connected to the nearest neighbor, unlike the actual microstructure of random fibrous network. These developed models however, are more suitable for fibrous network with local connections like pulmonary alveolus sac. Figure 5 below shows the SEM (Scanning Electron Microscope) image of the alveolar sac and the resulting FEM simulation done in [15]. Hence, the existing models are unable to simulate the non-local response of random fibrous network nor are they able to represent the actual fibrous microstructure.

This characteristics of the existing models leads to the two major objectives of this thesis

- Represent actual fibrous microstructure with non-local connections (if any).
- Simulate non-local response of random fibrous network.

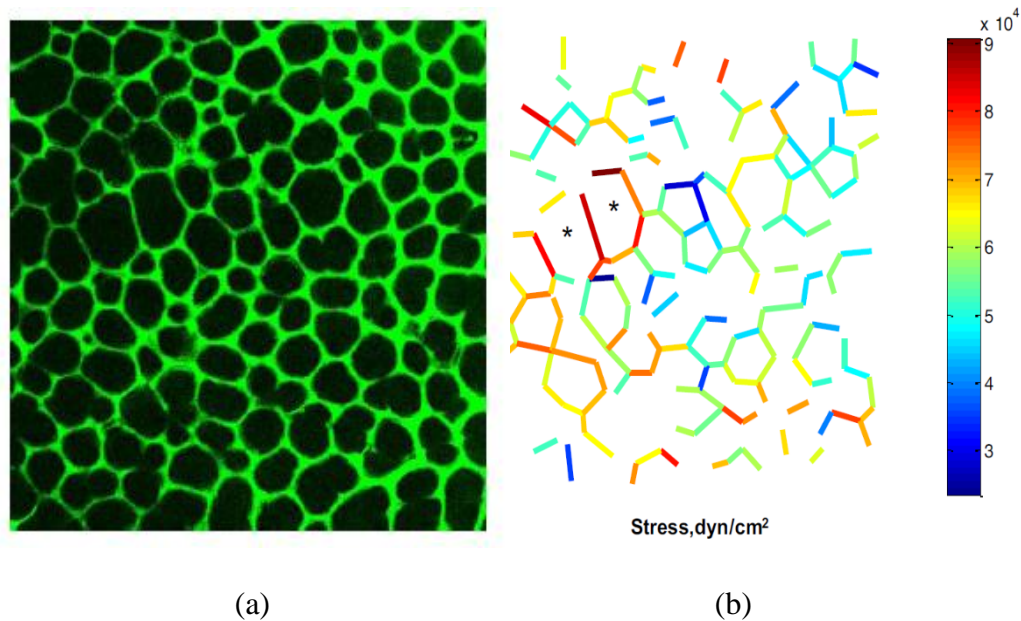


Figure 5: (a) Shows the SEM image of pulmonary alveolus sac. (b) Septal stress values in lung region of PTP (Pulmonary Transmissions Pressure) of 9 cm on deflation. The fibers were modelled as linear, fibers with unstressed length were omitted in the simulation [15]. This is a typical simulation of well-defined fibrous network as polygons. A single support will be modelled in this thesis in 3-D as a dodecahedron. *Large alveoli lacking cross bridges.

To model nonlocal deformation of random fibrous networks nonlocal continuum mechanics can be used. However, it still poses a challenge in mimicking the actual fibrous network and the differential equation obtained might be complicated with unknown boundary conditions. Alternatively, as a simple and more efficient way we can model fibrous network as a large deformation, non-local and non-linear truss network.

This thesis aims to answer the following research questions based on the hypothesis stated above.

1. How to model large deformation of fibrous network?

Fibrous networks can be modelled as a nonlinear truss network with large deformation. Large deformation of truss network is necessary since collagen fibers show deformation up to 30% [15]. Minimizing the potential energy is a simple method to solve the non-local problem in comparison to developing constitute equations based on non-local continuum mechanics.

2. How does macroscopic failure in fibrous network occur?

Studies have shown that there is a considerable difference between strains in individual fibers vs macroscopic average strain [10-16]. This disparity can be accounted for the non-local microstructure of random fibrous network. In this thesis, it is proposed that random fibrous network under uniaxial tension with non-local connections can be used to mimic ligament deformation.

3. How accurate are linear models for studying the failure of finite deformation?

Work done in [16, 18, and 19] have modelled the fibrous filaments with linear elastic material properties. A linear curve fit for the stress-strain response will be done and a linear model of the fibrous network will be done to compare accuracy with the non-linear simulations.

CHAPTER II

FIBROUS MATERIAL MODELLED AS A TRUSS NETWORK

One of the objectives of this thesis was to construct the actual non-local microstructure of the random fibrous network. In this chapter, the methodology used for generating random fibrous network will be discussed.

The microstructure of the random fibrous network will be represented by a non-local truss network. To generate the random truss network there are two requirements:

- Nodal locations: These represent the intersection of the filaments in the fibrous network.
- Nodal connections: These represent how the nodal locations identified will be connected.

The above two requirements will be discussed in detail in this chapter. The developed fibrous networks based and the algorithm to develop the network will be presented.

II.1 Generating Nodal Locations of Random Fibrous Network

Nodal locations represent the cross-link points in the actual fibrous network microstructure. Cross-link points are points where the filaments in the fibrous network intersect each other. The cross-link density depends on the actual material, not all overlapping fibers are fully bonded via a cross-link point but some fibers overlap and slide

across each other without friction. Figure 6 below shows the SEM (Scanning Electron Microscope) image of type 1 collagen fibers along with the cross-links identified.

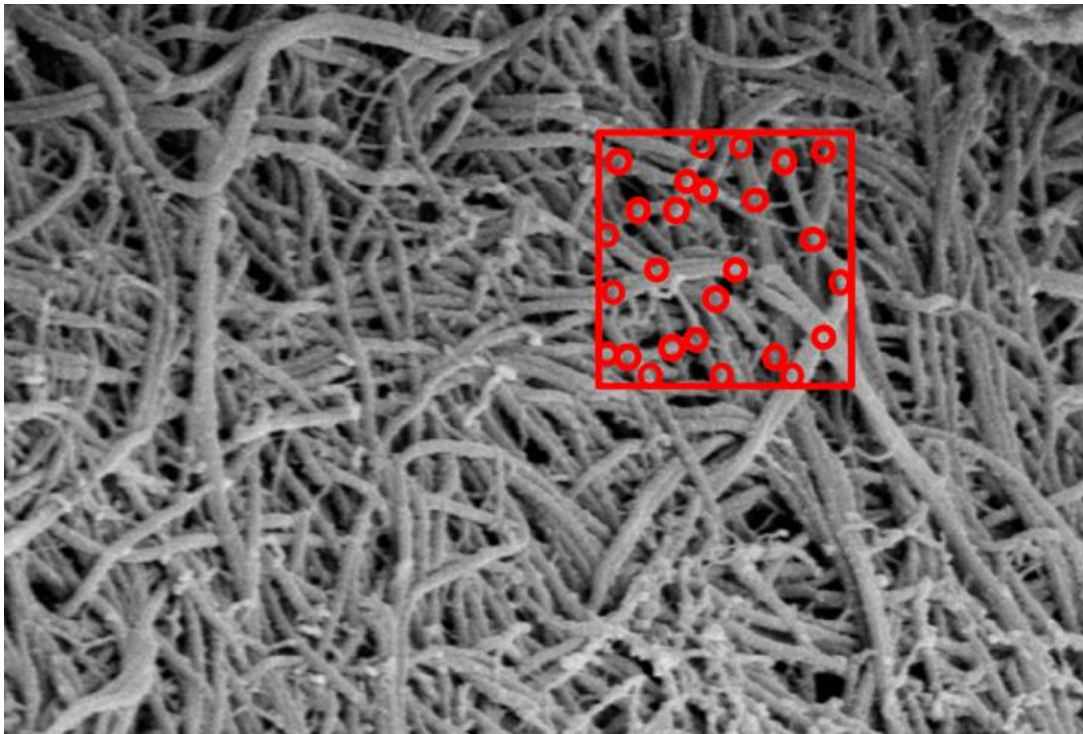


Figure 6: SEM of type 1 collagen fiber [22]. The red box represents the characteristic length of the matrix to be simulated. Locations where the fibers overlap are modelled as contact points. Fibers originating from these contact points overlapping other fibers in the model are assumed to be sliding over each other without friction.

As seen above in Figure 6, the nodal locations are identified from the above SEM image of type 1 collagen fibers. There are two methods to randomly generate nodes.

- Homogenous nodal locations
- Inhomogeneous nodal location

II.1.1 Homogenous Nodal Location Generation

The definition of homogenous nodal location used in this thesis is: the probability of finding a node is the same everywhere. If the actual microstructure of the fibrous network has cross-links that are homogeneously distributed. We can randomly generate the desired amount of points in the unit cell from a uniform probability distribution. This is accomplished in MATLAB by using the rand command.

II.1.2 Inhomogeneous Nodal Location Generation

In this thesis, inhomogeneous random points are generated from the probability distribution of the points originally identified in the microstructure. The probability of finding a node at a particular location is same as the probability distribution of the points in the original microstructure. Figure 7 (a) below shows the original nodes identified in the SEM (Scanning Electron Microscope) image and Figure 7(b) shows the random nodes generated from the probability distribution of nodes in 7(a). Figure 8 below shows the probability distribution of points in 7(a) for X & Y coordinate. A Kernel Epanechnikov probability function was used to fit that data, as it was a better fit than the normal distribution. Figure 9 below shows 1000 nodes generated from the probability distribution of 7(a). As seen in Figure 8, the points are in homogeneously distributed.

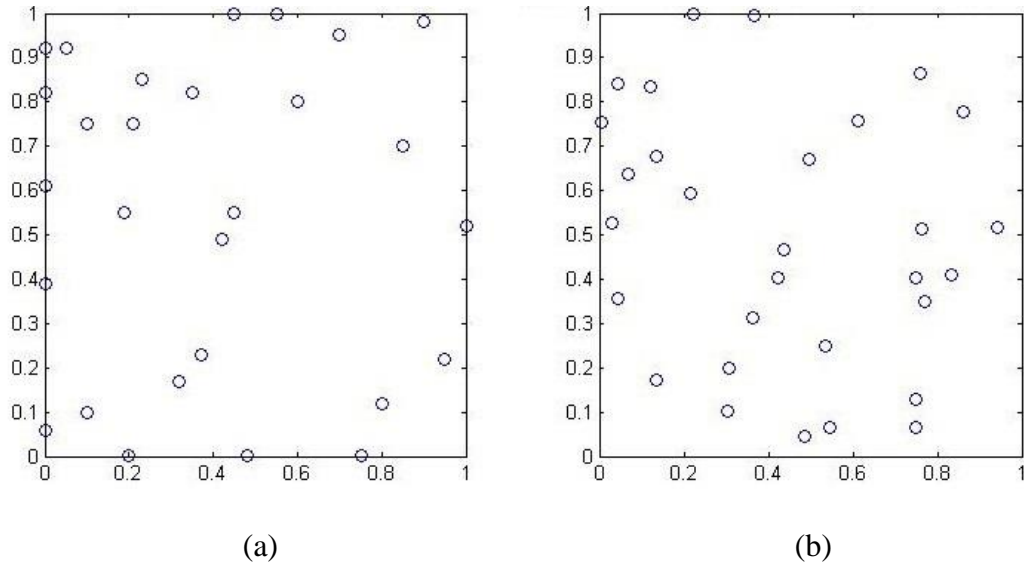


Figure 7: Random nodes generated from the PDF of the nodal connections identified in the SEM of fibrous network. (a) Shows originally identified nodes. (b) Shows nodes generated from (a).

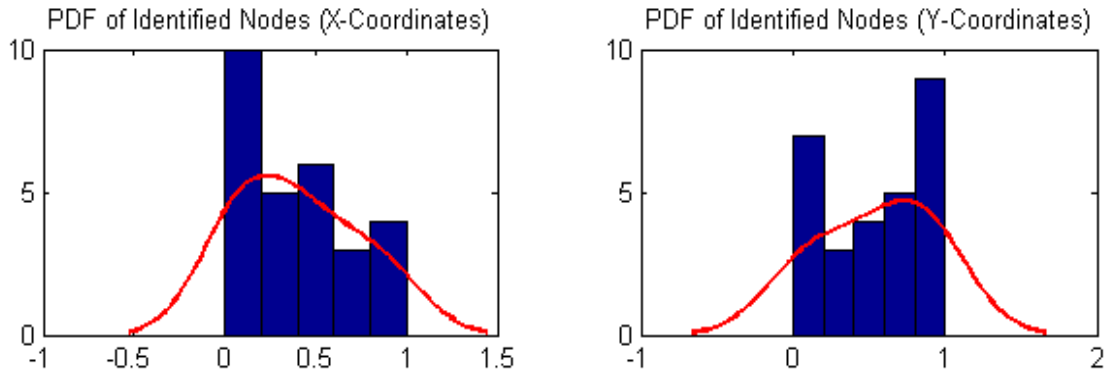


Figure 8: Probability distribution of points identified in 7(a). Kernel Epanechnikov probability distribution was found the best fit for the given data.

Figure 9 below shows 1000 nodes generated from the probability distribution of 7(a). As seen in Figure 8, the points are in homogeneously distributed. The algorithms for generating random fiber network are shown below in Appendix A.

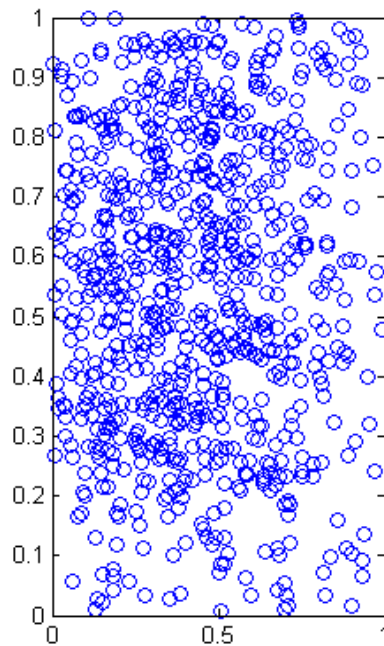


Figure 9: 1000 points generated from the probability distribution of points shown in Figure 8. The inhomogeneity in the distribution can clearly be seen as there are few points when $x=1$.

II.2 Generating Nodal Locations of Random Fibrous Network

Once the nodal locations have been generated in the matrix. The random fibrous network is finally formed by connected the nodes. This thesis proposes two major ways for forming nodal connections

- Symmetry
- Nodal location

Figure 10 below shows the flow chart developed for each connectivity method.

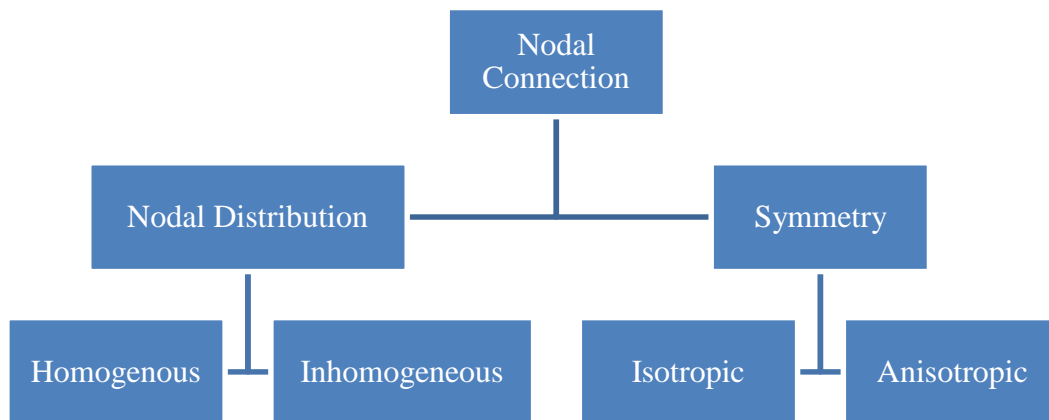


Figure 10: Flow charts developed for the two major categories for connecting random nodes generated.

The definition for each of the nodal connectivity categories is given below.

1. Nodal Distribution

- a. Inhomogeneous: The nodal connection depends on the location of the nodes (e.g.: preference is provided to connect points at a certain location than other points).
- b. Homogenous: The nodal connection is independent on the location of the nodes, i.e. preference is not given to the location of the nodes when connecting the network.

2. Symmetry

- a. Anisotropic: The nodal connection is based on distance/direction (e.g.: preference is given to connecting nodes that are below a certain angle).

- b. Isotropic: The nodal connection is independent of distance/direction. The connectivity is instead dependent on the probability distribution of number of nodal connections as a function of distance for every node. This is shown below in Figure 11.

As seen from Figure 10, there exists different ways of forming nodal connections. The following types of nodal connection combinations can be generated.

1. Homogenous and isotropic
2. Homogenous and anisotropic
3. Inhomogeneous and isotropic
4. Inhomogeneous and anisotropic

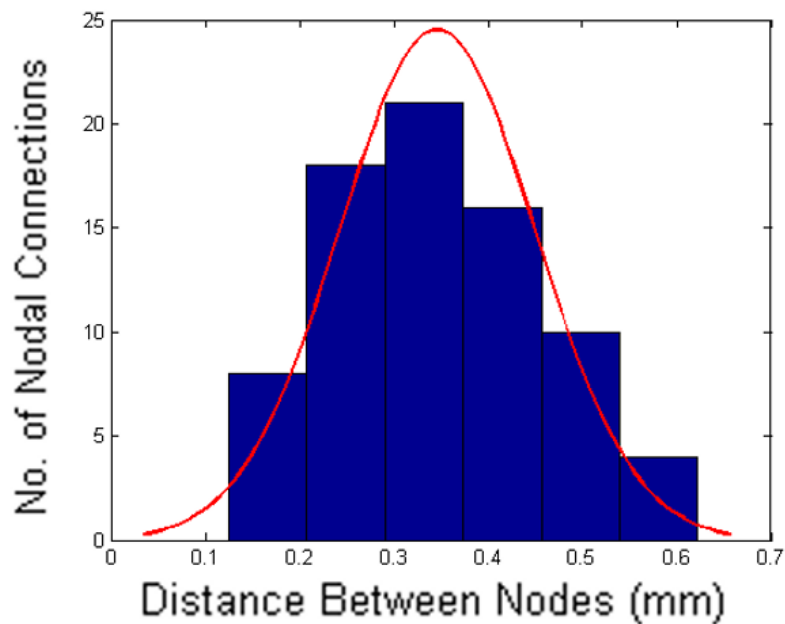


Figure 11: Probability distribution of nodal connections as a function of distance for nodes developed in 7(b).

Figure 12(a) below shows the homogenous and anisotropic and Figure 12 (b) shows the homogenous and isotropic connection for the random inhomogeneous nodes developed in Figure 7(b).

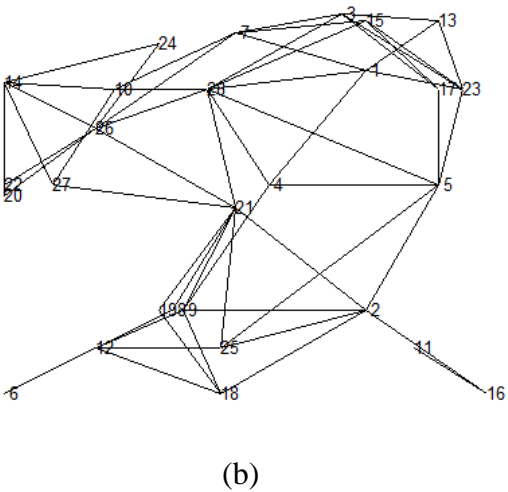
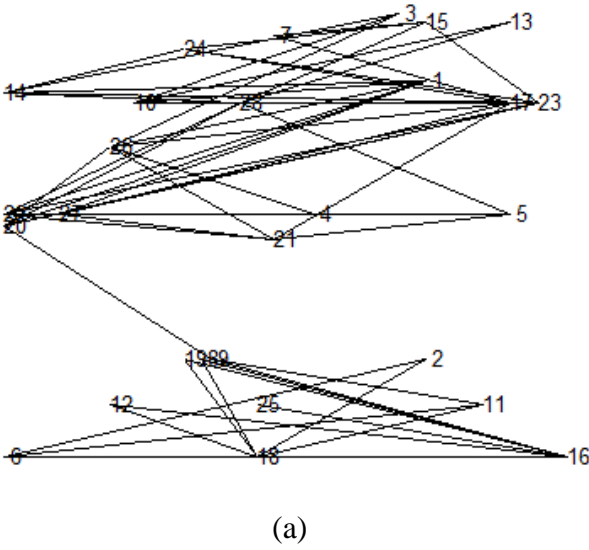


Figure 12: Non-local fibrous network developed from the SEM (Scanning Electron Microscope) image of type 1 collagen fiber in Figure 6. (a) Shows homogenous and anisotropic connection. (b) Shows homogenous and isotropic connection. The nodal points generated were inhomogeneous.

In Figure 12 (a), the connectivity method used to develop the network was homogenous and anisotropic. Only nodes that had an angle of less than 30° degrees were connected. The nodal connection was independent of the location of the nodes. Figure 12(b) the nodal connection were based on the probability distribution of number of nodal connections as a function of distance as shown in Figure 11.

As seen from above Figure 12, the non-local (fibers are connected to nodes far away from originating node) nature of the fibrous network was captured in the proposed method. For example in figure 12 (a), nodal connections between nodes 20 and 23 are non-local. In Figure 12(b) connections between 5 and 25 are non-local. Hence, the first major objective of replicating the microstructure of random fibrous network with non-local connections has been accomplished.

In the next chapter, the large and non-linear modelling of the developed truss network will be discussed.

CHAPTER III

ENERGY FORMULATION FOR THE TRUSS SYSTEM AND FINDING THE AVERAGE DEFORMATION GRADIENT

In the previous chapter, a generic fibrous material was represented by a network of randomly generated filaments forming a truss. This truss network is solved by assembling the summation of strain energy of each member and minimizing it to obtain the current nodal configuration of the system. In this chapter, the formulation of strain energy for the truss system, different measures of strain and finding the average deformation gradient to approximate the results as a continuum will be discussed.

III.1 Principle of Minimum Potential Energy

The statement of minimum potential energy is “When the total potential energy of the system is minimized, the system is in a state of stable static equilibrium.”

The potential energy function V of external forces F_i (external global point force), w (external distributed loads) acting on displacement (D_i and w) on the surface S of the elastic solid is given by equation (1).

$$V = \sum F_i D_i + \int_s w v \, dS \quad 3.1$$

Strain energy U is the energy stored by the system undergoing elastic deformation under an applied load. The strain energy density (strain energy per unit volume) is also

determined by the area under the stress strain curve. The equation for the strain energy is given below in in equation (2).

$$U = \int_v \int \sigma(\epsilon)^T d\epsilon dV \quad 3.2$$

The total potential energy is the difference between the strain energy U and the potential energy of external forces V . Minimizing this total potential energy for the non-linear elastic solid will give the equilibrium solutions to the random truss system developed in chapter II.

III.2 Relation between Engineering Strain and Green Lagrange Finite Deformation

To calculate the strain energy, finite deformation was used instead of engineering strain. However, the data in the papers presented in [15-17] the data given was in terms of engineering stress/strain. The following derivation provides insight into how the engineering strain was converted to Green-Lagrange strain for use in calculating the strain energy of the truss.

The stretch ratio of a differential element is defined be the following equation 3.3

$$\lambda_n = \frac{dx}{dX} \quad 3.3$$

where the dx is the deformed magnitude of the differential element in the reference configuration dX along the direction of the unit vector n . The engineering strain is given in the following equation 3.4 and it rewritten in terms of the stretch ratio defined above in equation 3.3

$$e_{\text{eng}} = \frac{dx-dX}{dX} = \lambda_n - 1 \quad 3.4$$

The Green-Lagrangian Strain Tensor is given by the following equation 3.5.

$$E = \frac{1}{2}(C-1) \quad 3.5$$

where E is the Green-Lagrangian Strain Tensor and C is the Cauchy-Green deformation tensor. The stretch ratio is also defined by Cauchy-Green deformation given below in equation 3.6

$$\lambda_n = \sqrt{C_{11}} \quad 3.6$$

Substituting equation 3.6 and 3.5 in 3.4 gives

$$e = \lambda_{11} - 1 = \sqrt{C_{11}} - 1 = \sqrt{1+2E_{11}} - 1 \quad 3.7$$

In the above equation solving explicitly for E (Green-Lagrangian Strain Tensor) in terms of engineering strain gives the final relation between E and e. The relation is given below in equation 3.9.

$$2E_{11} = \frac{(dx_1)^2 - (dX_1)^2}{(dX_1)^2} \quad 3.8$$

$$E_{11} = \left(\frac{dx_1 - dX_1}{dX_1} \right) + \frac{1}{2} \left(\frac{dx_1 - dX_1}{dX_1} \right)^2 = e + \frac{1}{2} e^2 \quad 3.9$$

III.3 Strain Energy Formulation for a Truss (2-D)

A generic truss with 3 members in its reference (material coordinates) configuration and current configuration (spatial coordinates) is shown below in Figure 13. For solving the truss problem in 2-D and surface mesh triangular elements were used. For solving truss problem in 3-D tetragonal elements were used.

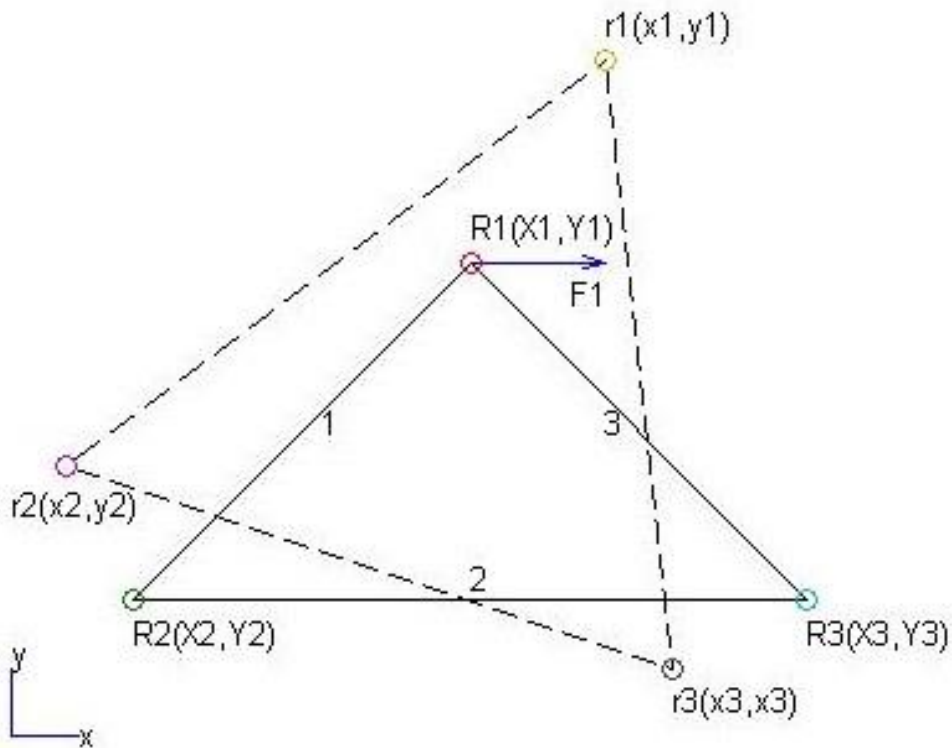


Figure 13: 2-D Truss with 3 members in reference and current configuration.
The dotted, straight lines represent current and reference configuration respectively

As seen from above in Figure 13, the member with a straight lines represent the truss in its material configuration and the members with dashed lines represent the truss in its spatial configuration. Each of global nodes represented by R1, r1, R2, r2, R3 and r3 have 2 local nodes in the coordinates x and y respectively.

III.3.1 Strain Energy of the Truss

Strain energy of the truss system given in above Figure 13 is given by the following equation 3.10. Note that all the strain given henceforth in the thesis are by default Green-Lagrange strain unless mentioned otherwise. The strain energy used below is an example of a strain energy ($U = \frac{1}{2}AE e^2$). However, the nonlinear case in which the strain energy will be of form $U = f(e)$ was developed and shown in a later section.

$$U = \frac{1}{2}AE (e_1^2 + e_2^2 + e_3^2) \quad 3.10$$

where e_1, e_2, e_3 represent the strain of each member in the truss in Figure 9. The strain of each member in the truss using equation 3.8 is given as:

$$2e_1 = \frac{\|r1-r2\|^2 - \|R1-R2\|^2}{\|R1-R2\|^2} \quad 3.11$$

$$2e_2 = \frac{\|r2-r3\|^2 - \|R2-R3\|^2}{\|R2-R3\|^2} \quad 3.12$$

$$2e_3 = \frac{\|r1-r3\|^2 - \|R1-R3\|^2}{\|R1-R3\|^2} \quad 3.13$$

where,

$$\|r1-r2\|^2=(x1-x2)^2+(y1-y2)^2 \quad 3.14$$

$$\|r2-r3\|^2=(x2-x3)^2+(y2-y3)^2 \quad 3.15$$

$$\|r1-r3\|^2=(x1-x3)^2+(y1-y3)^2 \quad 3.16$$

Similarly equations can be developed for the reference configuration $\{\|R1-R2\|, \|R2-R3\|, \|R1-R3\|\}$. These reference configuration value are provided by the user in the form of nodal values X_i, Y_i ($i=1:3$) and denote the square of length of each member. Substituting [3.11-3.16] in 3.10, the total strain energy of the system is given by 3.17.

$$U = \frac{1}{2} AE \left\{ \left[\frac{(x1-x2)^2+(y1-y2)^2 - \text{length}_1^2}{2\text{length}_1^2} \right]^2 + \left[\frac{(x2-x3)^2+(y2-y3)^2 - \text{length}_2^2}{2\text{length}_2^2} \right]^2 + \left[\frac{(x1-x3)^2+(y1-y3)^2 - \text{length}_3^2}{2\text{length}_3^2} \right]^2 \right\} \quad 3.17$$

These reference configuration value are provided by the user in the form of nodal values X_i, Y_i ($i = 1:3$). The potential energy function of the external forces is given by

$$V = F_{i(\text{Global})} X_i \quad 3.18$$

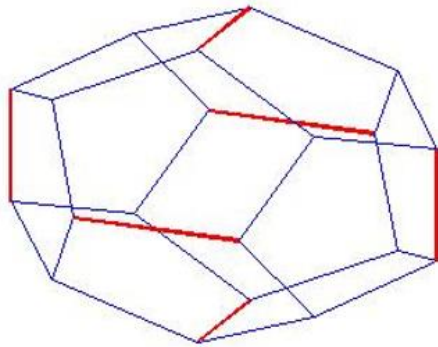
The potential energy for the Figure 9 is given by

$$V = F_1 x_1 \quad 3.19$$

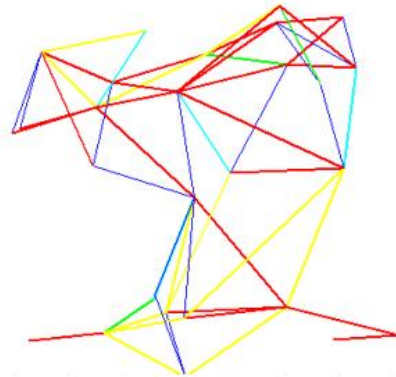
The required unknowns, current configuration values x_i, y_i are found by minimizing the total potential energy of the system as shown below

$$\Pi=U-V \quad 3.20$$

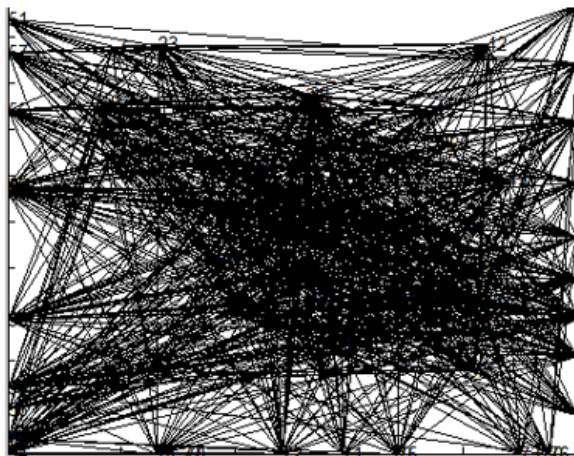
The minimization of 3.20 was done in MATLAB using fminunc function with quasi-newton algorithm. The algorithms for minimizing are shown below in Appendix B.



20 members-0.25 s



65 members-1.25 s



1000 members-4.75 s

Figure 14: Time taken to solve fibrous network along with the number of elements.

Figure 14 above shows the solver time taken for fibrous network with different element sizes. The quasi-newton algorithm is an alternative to newton's method and does not require jacobian/hessian input to minimize the objective function. If fibrous network of larger size (approx. 100,000) were to be minimized the jacobian could be assembled and provided to the solver for faster solving times.

III.4 Strain Energy for Linear and Non-Linear Response

One of the research questions to be answered was the accuracy of using strain energy of linear response in simulating the response of fibrous networks. The stress strain data obtained from [15]. The linear and non-linear curve fit of the stress-strain data is shown below in Figure 15. The linear model had a coefficient of determination (indication of how well the data fit the model) of 94% and the non-linear model has a coefficient of determination of 99%. Although there was only an error of 5% in choosing either of the models, significant difference in the simulation results for non-local random fibrous truss network was present, this is shown in detail later on in chapter IV. The quadratic strain energy strain energy derived by integrating the stress-strain response is shown below in Equation 3.21. The strain energy of the non-linear stress-strain response is shown below in Equation 3.22. Odd polynomials were used to model the non-linear stress-strain response.

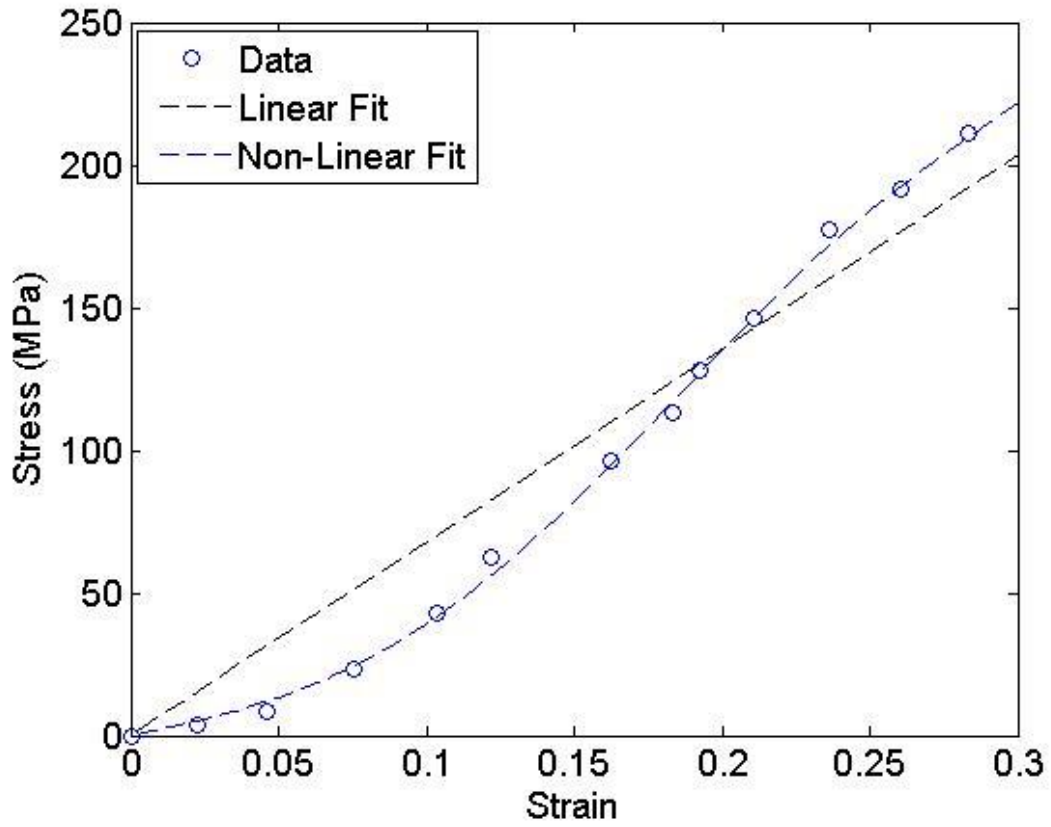


Figure 15: Linear and non-linear curve fit using odd polynomials of stress-strain data of individual collagen fibrils.

$$U=AL(339.75e^2) \quad 3.21$$

$$U=AL (1.249e^8-0.41e^6+.047e^4+.0011e^2) \times 10^5 \quad 3.22$$

where U refers to the strain energy, A refers to area, L refers to length of the fiber and e represents strain.

III.5 Finding Average Deformation Gradient

Another objective of this thesis was to compare the solution obtained if the fibrous network was modelled as a continuum. To obtain the approximate solution of the truss network as a continuum, the average deformation gradient was calculated from the exact solution found by minimizing the truss network using a least squares fit. The derivation of the average deformation gradient is shown below.

The solution of the truss network if modelled as a continuum is given by the following equation 3.23.

$$x_c = FX + B \quad 3.23$$

where x_c the solution if modelled as a continuum, F is the average deformation gradient, X is the reference configuration and B is the translation. The average deformation gradient is found by minimizing the following equation 3.24 with respect to the average deformation gradient F and translation B . x_t represents the solution found by minimizing the strain energy of the truss system.

$$\|x_c - x_t\|^2 \quad 3.24$$

Index notation will be used from here. For the i^{th} node the reference location is given as X^α and the truss solution for i^{th} node is given by x^α . Upon substituting 3.23 into 3.24 and minimizing with respect to F gives

$$\frac{\partial}{\partial F_{jp}} \sum_{\alpha} [F_{iA} X_A^\alpha + B_i - x_i^\alpha][F_{iA} X_A^\alpha + B_i - x_i^\alpha] = 0 \quad 3.25$$

$$\sum_{\alpha} [\delta_{ij} \delta_{AP} X_A^\alpha][F_{iB} X_B^\alpha + B_i - x_i^\alpha] + [F_{iA} X_A^\alpha + B_i - x_i^\alpha][\delta_{ij} \delta_{BP} X_B^\alpha] = 0 \quad 3.26$$

$$\sum_{\alpha} [F_{jB} X_B^{\alpha} + B_j - x_j^{\alpha}] X_p^{\alpha} = 0 \quad 3.27$$

$$F_{jB} \sum_{\alpha} X_B^{\alpha} X_p^{\alpha} + \sum_{\alpha} B_j X_p^{\alpha} + \sum_{\alpha} x_j^{\alpha} X_p^{\alpha} = 0 \quad 3.28$$

Upon replacing $\sum_{\alpha} X_B^{\alpha} X_p^{\alpha}$ with matrix M and $\sum_{\alpha} x_j^{\alpha} X_p^{\alpha}$ with N equation 3.28 can be written as

$$FM = N - BX^T \quad 3.29$$

Similarly upon minimizing equation 3.24 with respect to B gives.

$$\frac{\partial}{\partial B_j} \delta_{ij} [F_{iB} X_B^{\alpha} - B_i - x_i^{\alpha}] = 0 \quad 3.30$$

$$B = F \sum_{\alpha} X_B^{\alpha} - x_i^{\alpha} \quad 3.31$$

$$B = F \sum_{\alpha} X^{\alpha} - x^{\alpha} \quad 3.32$$

Hence, upon substituting 3.32 into 3.28, the average deformation gradient is found to be

$$FM = N - F \left[\sum_{\alpha} X^{\alpha} - x^{\alpha} \right] X^T \quad 3.33$$

Using the average deformation gradient found above in equation 3.33, the solution of the system if approximated as a continuum can be found and used for comparison purposes to the actual solution from the truss system. The following chapter IV and V show the simulations done for a local and non-local fibrous network using methodologies developed in this chapter.

CHAPTER IV

DEFORMATION OF A LOCAL SYSTEM

In this chapter, a locally connected system (where the nodes are connected only to the nearest neighbor) will be simulated and the following comparisons will be made in the results obtained

- Comparison between deformation mode in linear and non-linear system
- Compare truss solution to the solution obtained by approximating the system as a continuum.

IV.1 Locally Connected Fibrous Network of Pulmonary Alveolus Sac

Alveolus (Pulmonary alveolus) plays a major role in the operation of the lung, these hollow cavity like structures are found at the terminal ends of the respiratory systems in the lungs and are responsible for the gas exchange between the air in the lungs and the pulmonary capillaries. The surface of the alveolus is supported by a network of collagen fibers that closely resemble the shape of dodecahedron. These fibers are responsible for the elastic action of the alveolus during exhalation of air [14]. A typical alveoli with the supportive elastic fibrous structure is shown below in Figure 16.

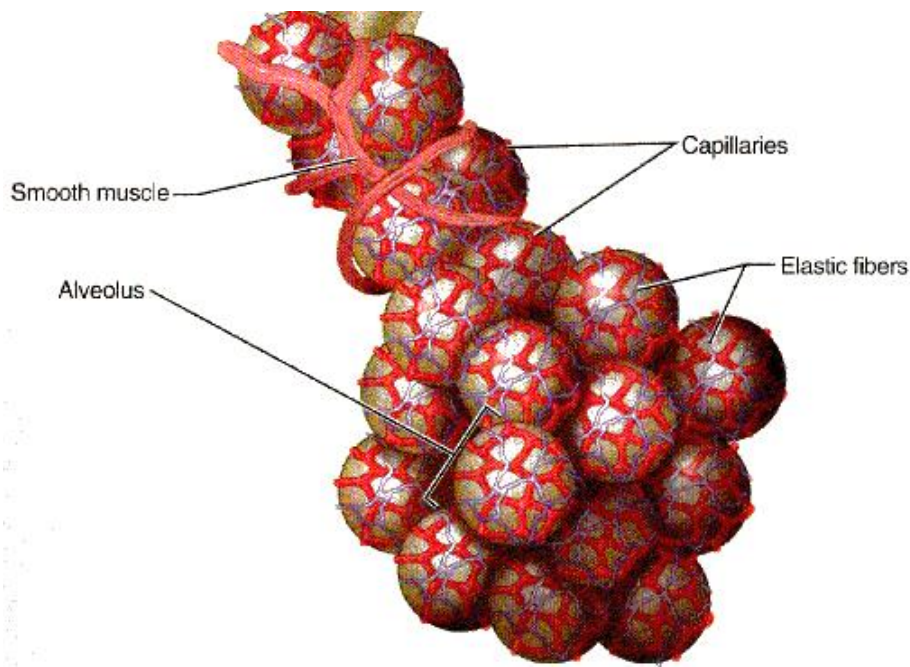


Figure 16: Alveoli structure, red bands show the elastic fiber support [13].

IV.1.1 Modelling an Alveolus Sac Elastic Support as a Dodecahedron

A single alveolus's (Pulmonary alveolus) elastic fiber support network was examined using a dodecahedron. A dodecahedron was chosen, since most lung studies modelled alveolus as a regular dodecahedron [23, 24]. The stress-strain data for the fibrils supporting the alveolar surface has been obtained from [15]. The dodecahedron had a volume of $8.735 \times 10^6 \mu\text{m}^3$ with an edge length of $104.6 \mu\text{m}$. Strain energy from equations 3.22 was used for modelling the non-linear response of the dodecahedron. Figure 17 shows the dodecahedron to be modelled. Radially expanding forces were applied from the middle of the dodecahedron to simulate expansion of alveolus sac.

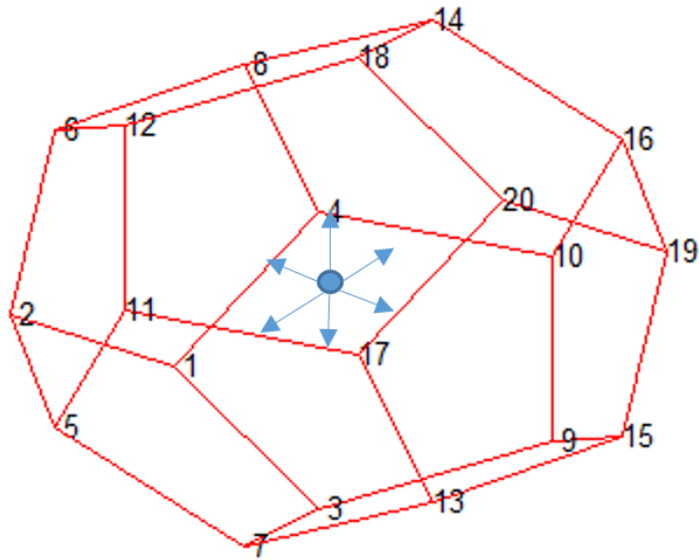


Figure 17: Elastic support of alveolus modelled as a dodecahedron.

Upon application of the forces the color coded deformation is shown below in Figure 18.

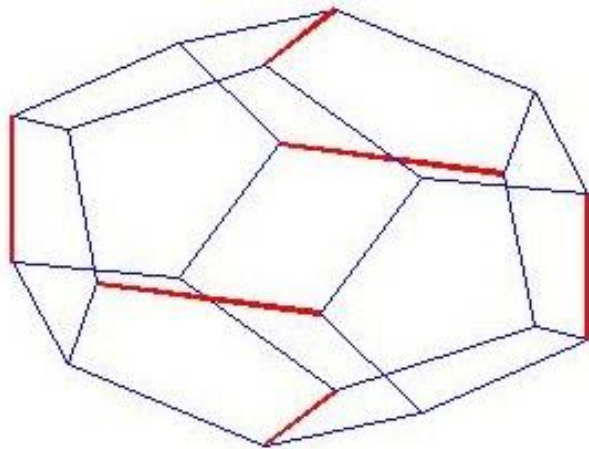


Figure 18: Repose of dodecahedron upon applying radially expanding forces from the centroid. Filaments in red experience higher strain than filaments in blue.

Figure 19 below shows the macroscopic strain, maximum and minimum microscopic strain of the dodecahedron computed for different loads applied evenly at the nodes to mimic the expansion of alveolus sac during inhalation of air.

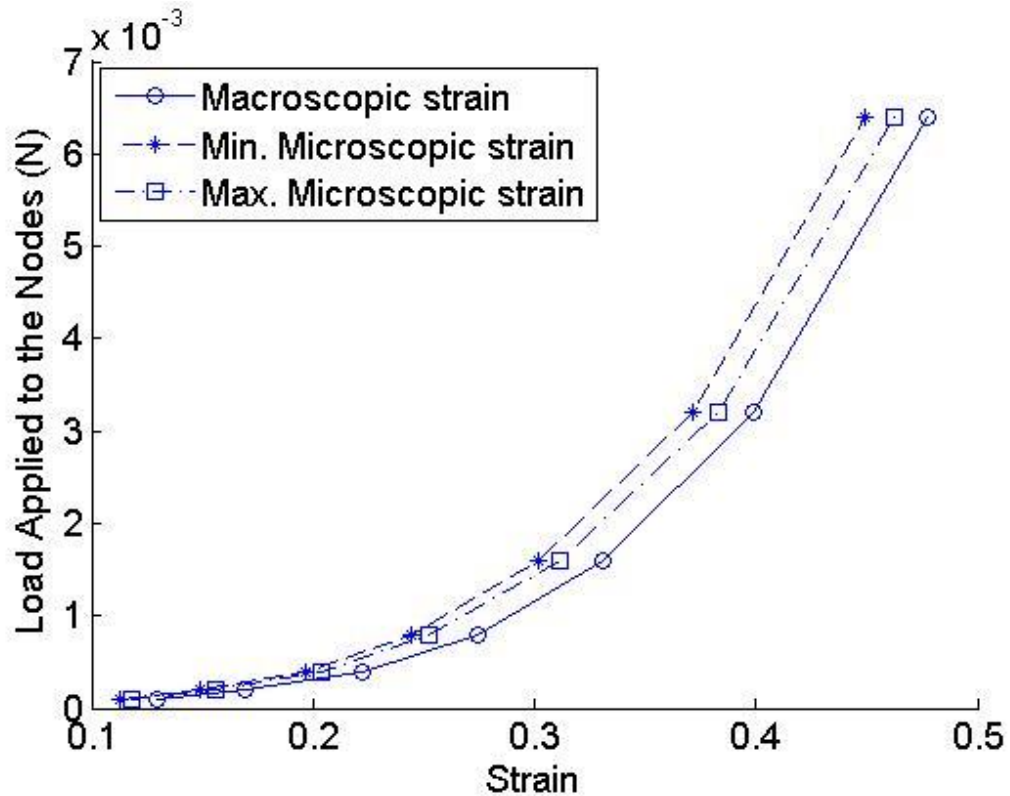


Figure 19: Macroscopic vs microscopic stress-strain of dodecahedron.

IV.2 Comparison between Deformation in Linear and Non-Linear Systems

The non-linear response has been modelled and is shown above in Figure 18 and 19. To simulate the response of the dodecahedron if it was assumed to have linear system, the strain energy in equation 3.21 was used. If the individual fibers were assumed to have linear stress-strain response, the deformation predicted by the linear response simulation was found to be the same as non-linear response simulation in Figure 18. Figure 20 below shows the maximum strain experienced by individual fibers in the dodecahedron.

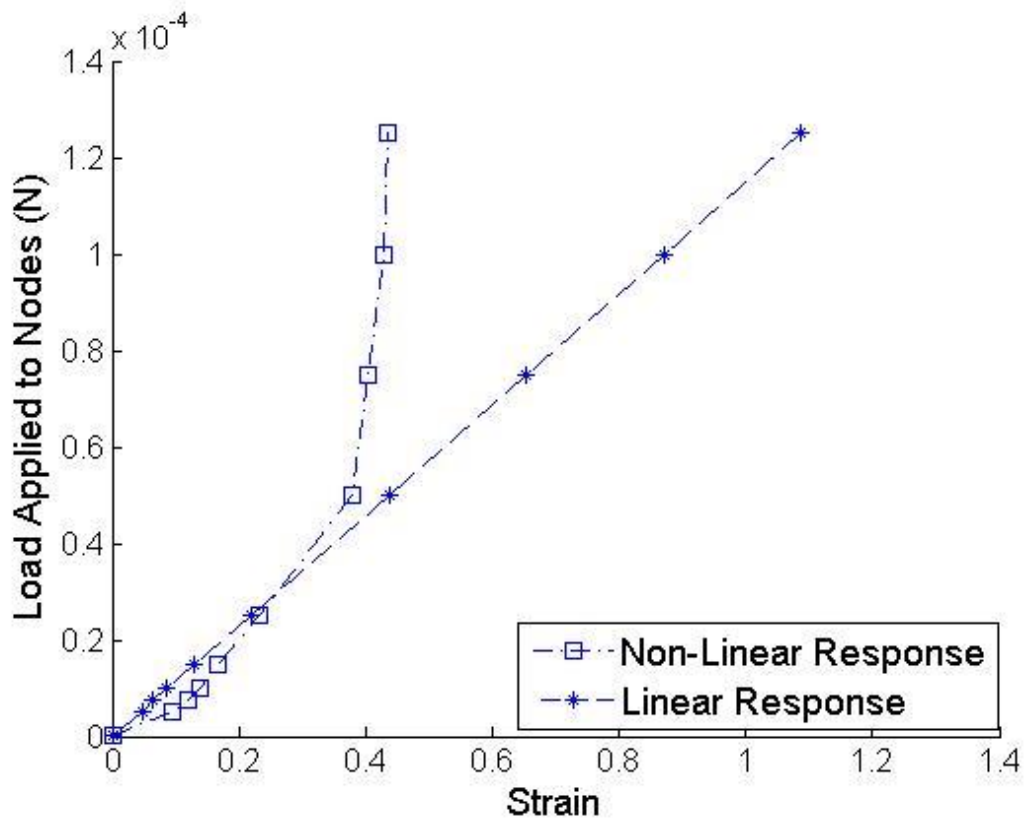


Figure 20: Maximum microscopic strain for linear and non-linear responses.

As seen from above Figure 20, modelling a local system using a linear response gives the same prediction as the non-linear response up to 30%. The deformation of individual fibers using a linear response was found to be the same as using non-linear response.

IV.3 Comparison between Deformation Predicted by Truss Network and Approximating as a Continuum

To compare the results if the system was approximated as a local continuum, the average deformation gradient was found using equation 3.33. From the average deformation gradient the solution of the system modelled as a continuum is calculated using equation 3.23. Figure 21 below shows the solution obtained by minimizing the strain energy (blue line) and the solution if approximated as a local continuum (red line).

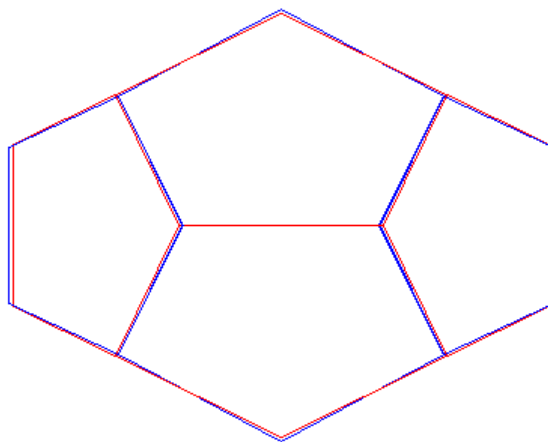


Figure 21: Shape of dodecahedron deformed by minimizing the strain energy (blue line) and approximating as a local continuum (red line).

For a local system, it was found that there were no significant differences between results obtained if linear response of fibers was used instead of non-linear response for up to 30% strain, as shown in Figure 20. Also, approximating the local system as a continuum exhibited no significant differences from if the system was instead modelled as a network of trusses, as shown in Figure 21. Hence, for a local system, modelling it as a simple local continuum with linear response fibers would have sufficed.

CHAPTER V

DEFORMATION OF A NON- LOCAL SYSTEM

In this chapter, a non-locally connected system (where the nodes can be connected to nodes far away from originating node) will be simulated and the following comparisons will be made in the results obtained

- Comparison between deformation mode in linear and non-linear system
- Compare truss solution to the solution obtained by approximating the system as a continuum.

The inhomogeneous, isotropic and non-local random fibrous network developed in Figure 12(b) is used in this chapter.

V.1 Comparison between Deformation in Linear and Non-Linear System Responses

The random fibrous network was modelled similar to chapter IV. The non-linear response was simulated using the strain energy presented in 3.22. The linear response was simulated using quadratic strain energy presented in 3.21. The random fibrous network was deformed by applying uniaxial tensile forces at the edges of the fiber mesh. Figure 22 below shows the percentage of fibers in the random fibrous network failing given a tensile load for linear and non-linear response. Failure is determined when the strain in the individual fiber exceeds 30%.

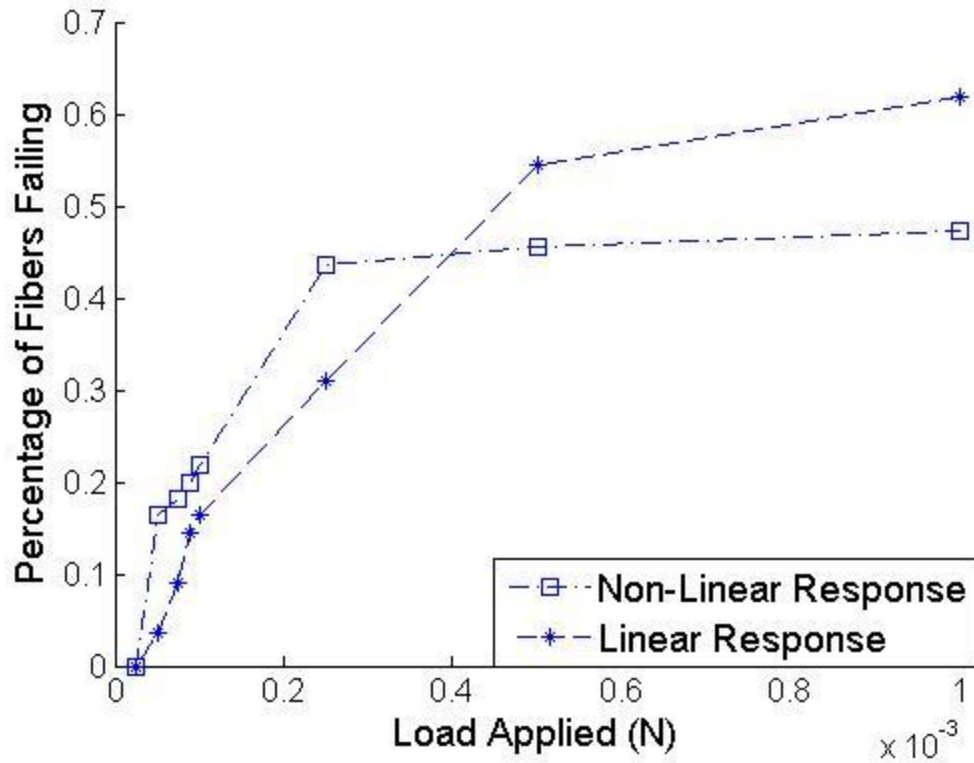


Figure 22: Percentage of fibers failing (strain>30%) given an applied load for linear and non-linear response.

The failure mode is also different for the linear and non-linear response. This is shown below in Figure 23 for an applied tensile load of 7.5e-4N. Unlike the local system in chapter IV, even for small loads there is a significant difference in the percentage of fibers failing as seen in Figure 22. Also the failure modes predicted by the linear response and non-linear response are entirely difference as seen in Figure 23.

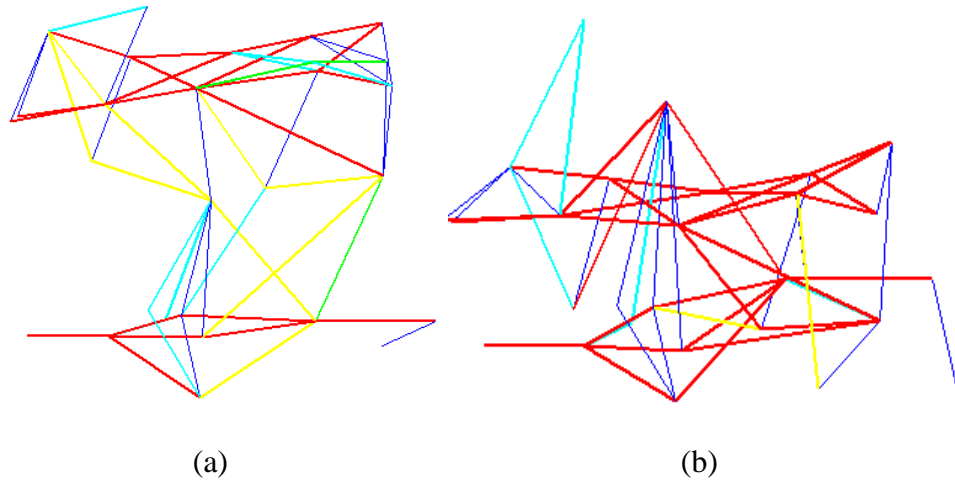


Figure 23: Deformation mode of linear (a) and non-linear (b) response given a tensile load of $7.45 \times 10^{-4} \text{ N}$.

V.2 Comparison between Deformation Predicted by Truss Network and Approximating as a Continuum

To compare the results if the system was modelled as a local continuum, the average deformation gradient was found using equation 3.33. From the average deformation gradient the solution of the system modelled as a continuum is calculated using equation 3.23. Figure 24 below shows the solution obtained by minimizing the strain energy (blue line) and the solution if approximated as a local continuum (red line).

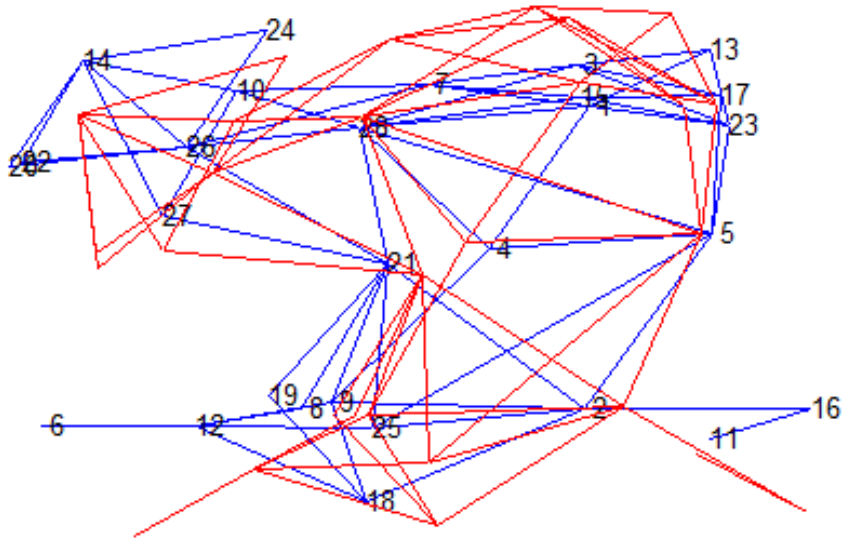


Figure 24: Deformed shape of dodecahedron by minimizing the strain energy (blue line) and approximating as a local continuum (red line).

Modelling the local system as a continuum exhibited no significant difference if the system was instead modelled as a network of trusses, as shown in Figure 24. To further quantify the difference continuum model and actual solution obtained by minimizing the potential energy of the truss network, a graph of actual strain vs average strain is calculated and is shown below in Figure 25. The average strain is calculated by using the following equation 5.1.

$$e_{\text{avg}} = \lambda^2 - 1 = E(F^T F)E^T - 1 \quad 5.1$$

where F is the average deformation gradient, E is the unit vector of each fiber.

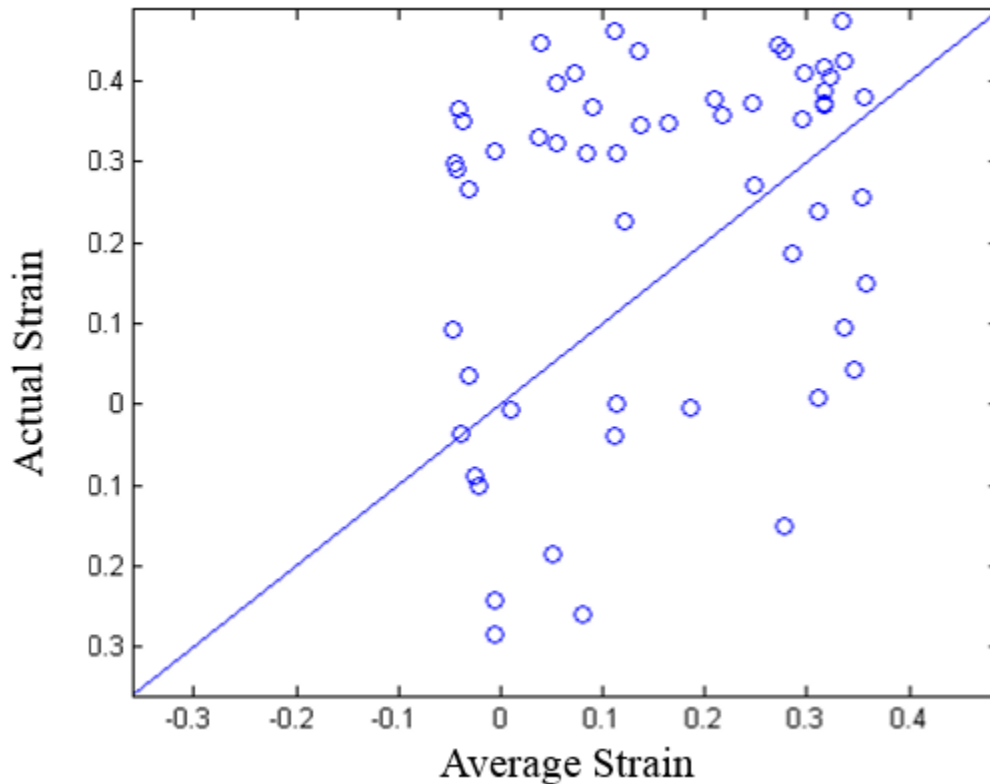


Figure 25: Plot of average strain calculated using the deformation gradient vs actual strain.

For a non-local system, it was found that there were significant differences between results obtained if linear response of fibers was used instead of non-linear, as shown in Figure 22. The deformation mode of non-local fibrous network was different for linear and non-linear response as shown in Figure 23. Also, approximating the local system as a continuum exhibited significant differences from if the system was instead modelled as a network of trusses, as shown in Figure 24. The plot of average strain calculated using the deformation gradient showed no correlation between average strain and actual strain found by minimizing the potential energy of the truss network as shown

in Figure 25. For a non-local system, modelling it as a simple local continuum with linear response fibers would not have sufficed. Hence, a non-local fibrous network has to be modelled as a network of trusses with non-linear response, where minimizing the total potential energy will provide solution to the system.

CHAPTER VI

CONCLUSION

In this work, fibrous networks have been modelled as a truss system with large deformation. The two major objectives of this work listed below have been met:

- Represent actual fibrous microstructure with non-local connections (if any).
- Simulate response of random fibrous network.

It has been shown than the actual microstructure of the fibrous network can be modelled as a network of trusses with non-local connections. The random fibrous networks were generated from the probability distribution of cross-linked identified in the SEM (Scanning Electron Microscope) image of the fibrous microstructure. The nodes were then connected by truss elements based on the probability distribution of number of nodal connections as a function of distance. Various other methods for developing random fibrous network have also been proposed in chapter 2.

The simulation of non-local response of random fibrous network was accomplished by minimizing the total potential energy of the system. Two types of fibrous networks were examined:

- Local system
- Non-local system

A pulmonary alveolus sac of human lung was modelled for the case of a local system. In the case of local system (network were fibers are connected to the nearest neighbor), it was found that there were no significant differences between results obtained

if linear response of fibers was used instead of non-linear response for up to 30% strain, as shown in Figure 20. Also, approximating the local system as a continuum exhibited no significant differences from if the system was instead modelled as a network of trusses, as shown in Figure 21. Hence, for a local system, modelling it as a simple local continuum with linear response fibers would have sufficed.

A non-local system of type 1 collagen fiber was generated using methods presented in chapter 2. For a non-local system, it was found that there were significant differences between results obtained if linear response of fibers was used instead of non-linear, as shown in Figure 22. The deformation mode of non-local fibrous network was different for linear and non-linear response as shown in Figure 23. Also, approximating the non-local system as a continuum exhibited significant differences from if the system was instead modelled as a network of trusses, as shown in Figure 24. The plot of average strain calculated using the deformation gradient showed no correlation between average strain and actual strain found by minimizing the potential energy of the truss network as shown in Figure 25. For a non-local system, modelling it as a simple local continuum with linear response fibers would not have sufficed. Hence, a non-local fibrous network has to be modelled as a network of trusses with non-linear response, where minimizing the total potential energy will provide solution to the system.

REFERENCES

- [1] K. K. Chawla, *Fibrous materials*. Cambridge, UK: Cambridge University Press, 2005.
- [2] S. P. Lake, K. S. Miller, D. M. Elliott, and L. J. Soslowsky, “Effect of fiber distribution and realignment on the nonlinear and inhomogeneous mechanical properties of human supraspinatus tendon under longitudinal tensile loading,” *Journal of Orthopaedic Research J. Orthop. Res.*, vol. 27, no. 12, pp. 1596–1602, 2009.
- [3] R. Fangueiro and S. Rana, “A Brief Review on the Latest Applications of Fibrous Materials in Advanced and Emerging Areas,” *J. Text. Eng. Journal of Textile Engineering*, vol. 59, no. 5, pp. 119–123, 2013.
- [4] A. M. Kiapour and M. M. Murray, “Basic science of anterior cruciate ligament injury and repair,” *Bone and Joint Research*, vol. 3, no. 2, pp. 20–31, 2014.
- [5] C. J. Mann, E. Perdiguero, Y. Kharraz, S. Aguilar, P. Pessina, A. L. Serrano, and P. Muñoz-Cánoves, “Aberrant repair and fibrosis development in skeletal muscle,” *Skeletal Muscle*, vol. 1, pp. 21–21, 2011.
- [6] A. Samani, J. Zubovits, and D. Plewes, “Elastic moduli of normal and pathological human breast tissues: an inversion-technique-based investigation of 169 samples,” *Physics in Medicine and Biology Phys. Med. Biol.*, vol. 52, no. 6, pp. 1565–1576, 2007.
- [7] S. E. Calvin and M. L. Oyen, “Microstructure and Mechanics of the Chorioamnion Membrane with an Emphasis on Fracture Properties,” *Annals of the New York Academy of Sciences*, vol. 1101, pp. 166–185, 2007.
- [8] N. M. Petri and D. Andri, “Differential Diagnostic Problems of Decompression Sickness—Examples from Specialist Physicians' Practices in Diving Medicine,” *Archives of Medical Research*, vol. 34, no. 1, pp. 26–30, 2003.

- [9] A. Ridruejo, C. González, and J. Llorca, “Micromechanisms of deformation and fracture of polypropylene nonwoven fabrics,” *International Journal of Solids and Structures*, vol. 48, no. 1, pp. 153–162, 2011.
- [10] G. N. Hermida, A. Far As, and L. E. Fiorito, “Neuroepithelial bodies in the lung of *Melanophryniscus stelzneri stelzneri* (Anura, Bufonidae),” *Anatomy and Embryology*, vol. 207, no. 4, pp. 373–379, 2003.
- [11] K. K. Brewer, H. Sakai, A. M. Alencar, A. Majumdar, S. P. Arold, K. R. Lutchen, E. P. Ingenito, and B. Suki, “Lung and alveolar wall elastic and hysteretic behavior in rats: effects of in vivo elastase treatment,” *Journal of Applied Physiology*, vol. 95, no. 5, pp. 1926–1936, 2003.
- [12] B. A. Roeder, K. Kokini, J. E. Sturgis, J. P. Robinson, and S. L. Voytik-Harbin, “Tensile Mechanical Properties of Three-Dimensional Type I Collagen Extracellular Matrices With Varied Microstructure,” *Journal of Biomechanical Engineering J. Biomech. Eng.*, vol. 124, no. 2, pp. 214–214, 2002.
- [13] K. K. Brewer, H. Sakai, A. M. Alencar, A. Majumdar, S. P. Arold, K. R. Lutchen, E. P. Ingenito, and B. Suki, “Lung and alveolar wall elastic and hysteretic behavior in rats: effects of in vivo elastase treatment,” *Journal of Applied Physiology*, vol. 95, no. 5, pp. 1926–1936, 2003.
- [14] C. E. Perlman and Y. Wu, “In situ determination of alveolar septal strain, stress and effective Young's modulus: an experimental/computational approach,” *AJP: Lung Cellular and Molecular Physiology*, vol. 307, no. 4, pp. 302-310, 2014.
- [15] Z. L. Shen, M. R. Dodge, H. Kahn, R. Ballarini, and S. J. Eppell, “Stress-Strain Experiments on Individual Collagen Fibrils,” *Biophysical Journal*, vol. 95, no. 8, pp. 3956–3963, 2008.
- [16] B. Sabuncuoglu, M. Acar, and V. V. Silberschmidt, “Finite element modelling of fibrous networks: Analysis of strain distribution in fibres under tensile load,” *Computational Materials Science*, vol. 79, pp. 143–158, 2013.

- [17] A. Kabla and L. Mahadevan, “Nonlinear mechanics of soft fibrous networks,” *Journal of The Royal Society Interface*, vol. 4, no. 12, pp. 99–106, 2006.
- [18] H. Hatami-Marbini, A. Shahsavari, and R. Picu, “Multiscale modeling of semiflexible random fibrous structures,” *Computer-Aided Design*, vol. 45, no. 1, pp. 77–83, 2013.
- [19] L. Zhang, S. P. Lake, V. H. Barocas, M. S. Shephard, and R. C. Picu, “Cross-linked fiber network embedded in an elastic matrix,” *Soft Matter*, vol. 9, pp. 6398–6398, 2013.
- [20] A. D’Amore, N. Amoroso, R. Gottardi, C. Hobson, C. Carruthers, S. Watkins, W. R. Wagner, and M. S. Sacks, “From single fiber to macro-level mechanics: A structural finite-element model for elastomeric fibrous biomaterials,” *Journal of the Mechanical Behavior of Biomedical Materials*, vol. 39, pp. 146–161, 2014.
- [21] N. Johnson and N. Thien, “Nonlocal Models in Continuum Mechanics,” *Advanced Computational Methods for Material Modeling*, edited by D.J. Benson and R.A. Asaro. ASME, vol. 180, pp. 59–70, 1993.
- [22] C. Koh and M. Oyen, “Branching toughens fibrous networks,” *Journal of the Mechanical Behavior of Biomedical Materials*, vol. 12, pp. 74–82, 2012.
- [23] A. Linhartov, W. Caldwell, and A. E. Andersonr, “A proposed alveolar model for adult human lungs: The regular dodecahedron,” *Anat. Rec. The Anatomical Record*, vol. 214, no. 3, pp. 266–272, 1986.
- [24] E. Kimmel and B. Budiansky, “Surface Tension and the Dodecahedron Model for Lung Elasticity,” *Journal of Biomechanical Engineering J. Biomech. Eng.*, vol. 112, no. 2, pp. 160–167, 1990.

APPENDIX A

In this appendix, the following supplementary material regarding generation of fibers network will be given.

- Algorithm for random node generation from a given set of nodes.
- Algorithm for generating random fibrous network.

A.1 Algorithm for Generating Random Nodes

The input to the program is the nodal coordinate of the nodes identified in the image. The following steps are taken by the program in generating the inhomogeneous random nodes.

1. Obtain nodal data from N.
2. Split the nodal data N into x and y coordinates array.
3. Use the 'fitdist' function in MATLAB to fit the given data to a probability distribution. MATLAB has various probability distribution fits to match the pattern of the given data. For example, normal fit for data that looks like a normal distribution, kernel Epanechnikov fit for data that looks like a kernel distribution. It is left to the discretion of the user to decide which preset fits their data accurately.
4. Obtain the probability distribution function using the command 'pdf' in MATLAB.
5. Generate random nodes from the probability distribution using the command 'random(pdf,N1)'. Where n1 represents the array of random numbers desired.

6. Remove all negative numbers from the generated random number if the user wants only positive coordinates.

A.1.2 Sample Code for Generating Random Nodes

```
%% Nodal data of the random mesh identified from the SEM image

nodaldata_mat=[ 1.0000    0.100    0.100; %% Step 1
 2.0000    0.0500    0.9200;
 3.0000    0.1000    0.7500;
 4.0000    0.1900    0.5500;
 5.0000    0.2100    0.7500;
 6.0000    0.2300    0.8500;
 7.0000    0.3500    0.8200;
 8.0000    0.3200    0.1700;
 9.0000    0.3700    0.2300;
10.0000    0.4200    0.4900;
11.0000    0.4500    0.5500;
12.0000    0.6000    0.8000;
13.0000    0.7000    0.9500;
14.0000    0.9000    0.9800;
15.0000    0.8500    0.7000;
16.0000    0.8000    0.1200;
17.0000    0.9500    0.2200;
18         .75      0.0001;
19         .48      0.0001;
20         .55      1;
21         1        0.52;
22         .0001    .39;
23         .0001    .61;
24         .0001    .92;
25         .0001    .82;
26         .0001    .06;
27         .45      1;
28         .2       0.0001;
]

x=nodaldata_mat(:,2); %% Step 2
y=nodaldata_mat(:,3);

plot(x,y,'o')

figure %% Step 3
pdx=fitdist(x,'Kernel','Kernel','epanechnikov')
pdy=fitdist(y,'Kernel','Kernel','epanechnikov')
```

```

X=pdf(pdx,x); %% Step 4
Y=pdf(pdy,y);

x2=random(pdx,[1,5000]) %% Step 5
y2=random(pdy,[1,5000])

final_x=[];
final_y=[];
for i=1:min(size(x2,2),size(y2,2))
    if x2(i)>0 && y2(i)>0 && x2(i)<=1 && y2(i) <=1
        final_x(i)=x2(i);
        final_y(i)=y2(i);
    end
end
final_x(final_x==0)=[];
final_y(final_y==0)=[];
figure
plot(final_x,final_y,'o')

```

A.2 Algorithm for Generating Random Fibrous Network

The input to the program is the nodal coordinate of the nodes generated from the previous program. The following steps are taken by the program in generating the inhomogeneous random nodes.

1. Obtain nodal data P (n x 3 array) from program in A1.
2. Obtain the probability distribution function as desired (if the user choose to generate isotropic network, then the PDF of number of nodal connections as a function of distance must be given). Else, the user can connect the nodes based on angle/distance between them. This will be shown below in section A.2.1 as the sample code.
3. Generate connectivity node based on the following for loop

4. Nested for loop start

4.1. For i=node 1: end node number

4.2. Generate random integer from [1-3]

4.3. For j= node 1:end node number

4.3.1. Case 1 (when random integer =1)

If length between nodes i&j is between mean-1*standard deviation of probability density function (pdf) node i & j are connected.

4.3.2. Case 2(when random integer =2)

If length between nodes i&j is between mean+1*standard deviation of probability density function (pdf) node i & j are connected.

4.3.3. Case 2(when random integer =2)

If length between nodes i&j is between mean-.5*standard deviation and .5* standard deviation of probability density function (pdf) node i & j are connected.

4.4 Close the double for loop

5. The output of this algorithm is the random connectivity member list

A.2.1 Sample Code for Generating Anisotropic Random Network

The following code shown below generate anisotropic network given the nodal data. The anisotropic network is generated by connected nodes within .25-.33 rad angle.

```
%% Nodal data of the random mesh identified from the SEM image
```

```
nodaldata_mat=[      1.0000      0.7500      0.8500;
    2.0000      0.7500      0.2200;
    3.0000      0.7000      1.0000;
    4.0000      0.5500      0.5500;
    5.0000      0.9000      0.5500;
    6.0000         0         0;
    7.0000      0.4800      0.9500;
    8.0000      0.3500      0.2200;
    9.0000      0.3700      0.2200;
   10.0000      0.2300      0.8000;
   11.0000      0.8500      0.1200;
   12.0000      0.1900      0.1200;
   13.0000      0.9000      0.9800;
   14.0000         0      0.8200;
   15.0000      0.7500      0.9800;
   16.0000      1.0000         0;
   17.0000      0.9000      0.8000;
   18.0000      0.4500         0;
   19.0000      0.3200      0.2200;
   20.0000         0      0.5200;
   21.0000      0.4800      0.4900;
   22.0000         0      0.5500;
   23.0000      0.9500      0.8000;
   24.0000      0.3200      0.9200;
   25.0000      0.4500      0.1200;
   26.0000      0.1900      0.7000;
   27.0000      0.1000      0.5500;
   28.0000      0.4200      0.8000;
```

```
]
%% Splitting nodal matrix into x & y array
p=[];
p(:,1)=[1:1:28]';
p(:,2)=nodaldata_mat(:,2)
p(:,3)=nodaldata_mat(:,3)
x = p(:,2);
y = p(:,3);

%% For loop for connecting nodes based on vertical angle

for i=1:size(p,1)

%%Generating a random number from 1-5 to create randomness.

    a=randi([1,5])
```

```

    %% Nested for loop to match each node with other nodes and compare
    angles
    for j=1:size(p,1)
        length=sqrt( (p(i,2)-p(j,2))^2+(p(i,3)-p(j,3))^2);

%%case 1
        if a==1

            if abs((p(i,3))-p(j,3))<0.25
                avglength(i1)=length
                t2(i1,1)=i1;
                t2(i1,2)=i;
                t2(i1,3)=j;
                i1=i1+1;
            end
        end

%% case 2
        if a==2

            if abs((p(i,3))-p(j,3))<0.3
                avglength(i1)=length
                t2(i1,1)=i1;
                t2(i1,2)=i;
                t2(i1,3)=j;
                i1=i1+1;

            end
        end

%% case 3
        if a==3

            if abs((p(i,3))-p(j,3))<0.27
                avglength(i1)=length
                t2(i1,1)=i1;
                t2(i1,2)=i;
                t2(i1,3)=j;
                i1=i1+1;

            end
        end

%% case 4
        if a==4

```

```

        if length>=m+s && length<=m+2*s
            if length>0
                if abs((p(i,3))-p(j,3))<0.35
                    avglength(i1)=length
                    t2(i1,1)=i1;
                    t2(i1,2)=i;
                    t2(i1,3)=j;
                    i1=i1+1;
                end
            end
        end
%% case 5
        if a==5

            if abs((p(i,3))-p(j,3))<0.33
                avglength(i1)=length
                t2(i1,1)=i1;
                t2(i1,2)=i;
                t2(i1,3)=j;
                i1=i1+1;
            end
        end
    end

end

t5=[];
t5=t2;
temp=[];
temp(:,1)=t2(:,2);
temp(:,2)=t2(:,3);
%% Sorting to prevent repetitive entries.
temp=unique(sort(temp,2), 'rows');
t6=[];
t6=temp;
sizt2=size(temp,1);
t2=zeros(sizt2,3);
t2(:,1)=[1:1:sizt2]';
t2(:,2)=temp(:,1);
t2(:,3)=temp(:,2);

%% Finally creating matrix showing the nodes each member is connected
to
memberdata_mat=t2;

```


APPENDIX B

In this appendix, the following supplementary material for assembling the strain energy of the truss system and solving it.

- Algorithm for assembling the strain energy of the system and minimizing it.
- Forces applied to the dodecahedron to deform it.

B.1 Strain Energy Assembly Algorithm

To formulate the strain energy of a large truss system an automated algorithm was generated programmed.

Note: They user has the option to either supply the program with the following inputs, or use the existing random mesh program algorithm shown in chapter 2 .

Input If user choose to enter data manually:

1. Nodal matrix ($n \times 3$ or $n \times 4$ array for 2-D and 3-D respectively) containing node number and coordinate position.
2. Connectivity matrix ($n \times 2$ array)
3. Force matrix ($n \times 3$ or $n \times 4$ array for 2-D and 3-D respectively) containing force magnitude and direction applied at a node.
4. Constrained node matrix ($n \times 3$) containing node list and nodes being constrained.

Output The program gives the list of current nodal data, by minimizing the strain energy

Algorithm

1. Using nodal data and member connectivity data, find the length of each member.

The length of the each member is required to find the strain. The length is found by calculating the distance between two nodes given in the connectivity matrix by the following matrix in a for loop

for i=1: size of connectivity matrix

$$x_i = \text{NodaldataMatrix}(\text{Connectivity Matrix } (i,2),2);$$

$$x_{i+1} = \text{NodaldataMatrix}(\text{ConnectivityMatrix}(i,3),2);$$

$$y_i = \text{NodaldataMatrix}(\text{Connectivity Matrix } (i,2),3);$$

$$y_{i+1} = \text{NodaldataMatrix}(\text{ConnectivityMatrix}(i,3),3);$$

$$z_i = \text{NodaldataMatrix}(\text{Connectivity Matrix } (i,2),3);$$

$$z_{i+1} = \text{NodaldataMatrix}(\text{ConnectivityMatrix}(i,3),3);$$

$$\text{length}(i) = \text{sqrt}((x_{i+1} - x_i)^2 + (y_{i+1} - y_i)^2 + (z_{i+1} - z_i)^2);$$

end

2. The values supplied by the user in the force matrix and constraint matrix are in terms of global nodes. Each global node R_i has 3 local nodes (x_i, y_i, z_i) associated with it in 3-D and 2 local nodes in 2-D (x_i, y_i) . For example, the user specifies a force is applied at node R1 with magnitude M_x, M_y and M_z in the (x,y,z) direction. However, the strain energy being minimized utilizes local nodes indices. The relationship between global nodes and local nodes in 3-D is given by the following equation (B.1-B.5).

$$x_i = 3R_i - 2 \quad B.1$$

$$y_i = 3R_i - 1 \quad B.2$$

$$z_i = 3R_i \quad B.3$$

The relationship between global nodes and local nodes in 2-D is given by the equations (B.4-B.5)

$$x_i = 2R_i - 1 \quad B.4$$

$$y_i = 2R_i \quad B.5$$

3. The potential energy function for external forces is calculated by the following for loop

```
forcefunction=[];
```

```
For i=1:size of ConnectivityMatrix
```

```
f= local node index number* global force value;
```

```
forcefunction=forcefunction+f;
```

```
End
```

The local node index number is calculated by the relations given above. Similarly using the above for loop the strain energy for each member in the truss network is calculated (refer equations 3.17-3.20).

4. The constrained nodal value is replaced in the above function with the value given in Nodal Matrix. Using find function in MATLAB.

5. The initial value to be supplied to the minimizer is converted from a [nx3] array to [1xn] array using the following for loop

```
For i=1:size of Nodal Matrix
```

```
j=1;
```

```
int(j)=NodalMatrix(i,2);
```

```
int(j+1)=NodalMatrix(i,3);
```

```
int(j+2)=NodalMatrix(i,4);
```

```
j=j+3;
```

```
end
```

6. The total potential energy is then formulated according to equation 3.20 and minimized using the following command in matlab

```
[x_new]=fmiunc(total potential function,initial value)
```

7. Plot old and new members using the line command

Summary of algorithm

1. Accept input from randommesh program presented in chapter 2, force and constrained node details OR in addition to force and constrained nodes, accept Nodal matrix and connectivity
2. Find length of given members
3. Convert given global nodal coordinates to local coordinates
4. Construct total potential energy of the system by running the for loop command for external force function and strain energy function of the truss.

5. Replace the constrained nodal indices given by the user with the value from Nodal Matrix.
6. Initial value array [1 xn] is created by converting the Nodal Matrix [nx3] array
7. New location of the nodes is found by utilizing the matlab solver fminunc.
8. Plot Data

B.1.1 Sample Code of a Dodecahedron

The following myfun function assembles the strain energy

```
function [ f ] = myfun( x,m_dat,f_mat,length )

%%Description of Variables Used
%% X= Objective function var, m_dat= Nodes each member is connected to
%% f_mat=external forces applied. Length=length of each truss element
f1=0;

m=size(f_mat,1);

%%Assembling strain energy due to external forces %%%

for i=1:m
    f2=x(3*f_mat(i,1)-2)*f_mat(i,2)+x(3*f_mat(i,1)-
1)*f_mat(i,3)+x(3*f_mat(i,1))*f_mat(i,4);
    f1=f1+f2;
end

size_plot=size(m_dat,1);

%%Assembling strain energy of the members %%%
%Strain energy form U=(.016Xe8-.00538Xe6+6.4e-4Xe4+1.4e-5Xe2)Length

j=1;

h1=0;
```

```

for i=1:size_plot
    h2=(length(j)*.016*((x(3*m_dat(i,2))-x(3*m_dat(i,3))-2)-x(3*m_dat(i,3)-2))^2
+ (x(3*m_dat(i,2))-1)-x(3*m_dat(i,3)-1))^2 + (x(3*m_dat(i,2))-
x(3*m_dat(i,3)))^2 -length(j)^2)/length(j)^2)^8+length(j)*-5.385*10^-
3*((x(3*m_dat(i,2))-2)-x(3*m_dat(i,3)-2))^2 + (x(3*m_dat(i,2))-1)-
x(3*m_dat(i,3)-1))^2 + (x(3*m_dat(i,2))-x(3*m_dat(i,3)))^2 -
length(j)^2)/length(j)^2)^6 +length(j)*6.4*10^-4*((x(3*m_dat(i,2))-2)-
x(3*m_dat(i,3)-2))^2 + (x(3*m_dat(i,2))-1)-x(3*m_dat(i,3)-1))^2 +
(x(3*m_dat(i,2))-x(3*m_dat(i,3)))^2 -length(j)^2)/length(j)^2)^4 +
length(j)*1.4*10^-5*((x(3*m_dat(i,2))-2)-x(3*m_dat(i,3)-2))^2
+ (x(3*m_dat(i,2))-1)-x(3*m_dat(i,3)-1))^2 + (x(3*m_dat(i,2))-
x(3*m_dat(i,3)))^2 -length(j)^2)/length(j)^2)^2);
j=j+1;
h1=h1+h2 ;
end

f= -f1+h1;

end

```

The following script calls the assembly function and minimizes the strain energy.

```

%%Data Entry
%% Supply Location of nodes, forces applied, member connected to which
%%nodeand constrained node.

nodaldata_mat=p1;
memberdata_mat=t1;
n=size(memberdata_mat,1);
p=nodaldata_mat;
removaldata_mat=[];

%%%%%%%%%%%%Start Simulation for new nodes%%%%%%%%%%%%
%memberdata_mat=t1

%%Forces being applied to dodecahedron

fx= 2*10^-2;
f_mat=[1 -fx 0 0; 2 -fx 0 0; 20 fx 0 0; 19 fx 0 0; 12 0 fx 0; 11 0 fx 0
; 10 0 -fx 0; 9 0 -fx 0; 13 0 0 -fx; 7 0 0 -fx; 14 0 0 fx; 8 0 0 fx;
    3 -.5*fx -.5*fx -.5*fx;
    5 -.5*fx .5*fx -.5*fx;
    15 .5*fx -.5*fx -.5*fx;
    17 .5*fx .5*fx -.5*fx;
    4 -.5*fx -.5*fx .5*fx;
    6 -.5*fx .5*fx .5*fx;
    16 .5*fx -.5*fx .5*fx;

```

```

        18 .5*fx .5*fx .5*fx];
j=1;
n=size(memberdata_mat,1);

%% plotting dodecahedron to show to the user.
x_plot=[];
y_plot=[];
z_plot=[];
length=[];
m=size(f_mat,1);

for i=1:1:n

    x_a=nodaldata_mat(memberdata_mat(i,2),2);
    x_b=nodaldata_mat(memberdata_mat(i,3),2);
    y_a=nodaldata_mat(memberdata_mat(i,2),3);
    y_b=nodaldata_mat(memberdata_mat(i,3),3);
    z_a=nodaldata_mat(memberdata_mat(i,2),4);
    z_b=nodaldata_mat(memberdata_mat(i,3),4);

    x_plot(j)=nodaldata_mat(memberdata_mat(i,2),2);
    x_plot(j+1)=nodaldata_mat(memberdata_mat(i,3),2);
    y_plot(j)=nodaldata_mat(memberdata_mat(i,2),3);
    y_plot(j+1)=nodaldata_mat(memberdata_mat(i,3),3);
    z_plot(j)=nodaldata_mat(memberdata_mat(i,2),4);
    z_plot(j+1)=nodaldata_mat(memberdata_mat(i,3),4);
    j=j+2;

    length(i)=sqrt( (x_a-x_b)^2+(y_a-y_b)^2 + (z_a-z_b)^2);

end

%% Formulating the initial conditions
int=[];
n=size(nodaldata_mat,1)
j=1;

for i=1:n

    int(j)=nodaldata_mat(i,2);
    int(j+1)=nodaldata_mat(i,3);
    int(j+2)=nodaldata_mat(i,4);
    j=j+3;
end
m_dat=memberdata_mat

%%Calling the myfun function defined above & minimizing

f=@(x)myfun( x,m_dat,f_mat,length)
[x0,fval] = fminunc(f,int);

```

```
n=size(nodaldata_mat,1);
new_nod=zeros(n,4);

%% Using the values obtained to construct a new nodal matrix
%%containing the node value and the coordinates associated with it

for i=1:n
    new_nod(i,1)=i;
    new_nod(i,2)=x0(3*i-2);
    new_nod(i,3)=x0(3*i-1);
    new_nod(i,4)=x0(3*i);
end
```